

AD-A155 187

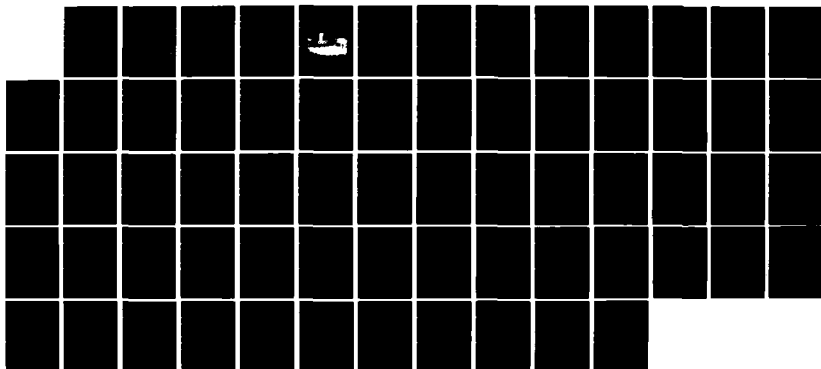
FLIGHTCONTROL SYSTEM FOR A COMPUTER CONTROLLED
AIRCRAFT WITH LIMITED SENSORS(U) AIR FORCE ACADEMY CO
T P WEBB 30 APR 85 USAFA-TN-85-4

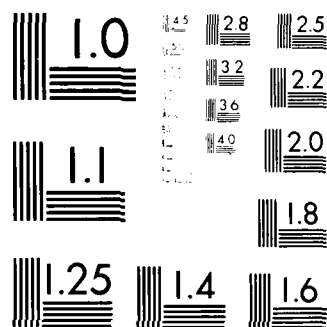
1/1.

UNCLASSIFIED

F/G 1/4

NL





MICROCOPY RESOLUTION TEST CHART
NATIONAL BUREAU OF STANDARDS-1963-A

2



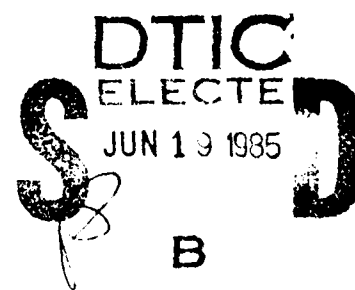
Department of Aeronautics
Dean of the Faculty
United States Air Force Academy
Colorado 80840-5831

AD-A155 107

FLIGHT CONTROL SYSTEM FOR A COMPUTER
CONTROLLED AIRCRAFT WITH LIMITED SENSORS

TECHNICAL NOTE
USAFA-TN-85-4

Webb, T.P.



DTIC FILE COPY

30 APRIL 1985

APPROVED FOR PUBLIC RELEASE: DISTRIBUTION UNLIMITED

85 5 21 006

Any views expressed in this paper are those of the author. They should not be interpreted as reflecting the views of the USAF Academy or the official opinion of any governmental agency. Notes are not reviewed for content or quality by the USAF Academy but are published primarily as a service to the faculty to facilitate internal research communication.

This Technical Note has been cleared for open publication and/or public release by the appropriate Office of Information in accordance with AFR 190-17 and DODD 5230.9. There is no objection to unlimited distribution of this Technical Note to the public at large or by DDC to the National Technical Information Service.

This Technical Note is approved for publication.



Thomas E. McCann, Lt Colonel, USAF
Director of Research and Computer Based Education

✓	
PER CALL JC	
A-1	



FLIGHT CONTROL SYSTEM DESIGN FOR A COMPUTER CONTROLLED AIRCRAFT WITH LIMITED SENSORS

Thomas P. Webb*

Abstract

A complete flight control system for a small computer controlled aircraft was designed using only yaw rate, heading, lateral load factor, airspeed, altitude, and rate of climb feedback. This multi-input multi-output control problem was done using the classical root locus technique on a linearized system model. The performance of the flight control system was then checked using a 12 degree-of-freedom nonlinear simulation. The simulation results revealed surprisingly good performance, considering the limitation on sensors.

I. Introduction

The Department of Electrical Engineering at the United States Air Force Academy is attempting, through one of its senior design courses, to design, build, and fly a computer controlled aircraft. The Department of Aeronautics was asked to help design the flight control system to be implemented by the on-board digital computer. The project involved building and testing a wind tunnel model of the aircraft to determine its aerodynamic characteristics, performing mass tests on the actual aircraft to determine inertia characteristics, developing a 12 degree-of-freedom nonlinear aircraft simulation program, and designing the actual flight control system. This report describes only the last task.

II. Aircraft Description

The aircraft acquired by the Electrical Engineering Department is an off the shelf hobby radio controlled airplane called the "Big Stick" sold by Hobby Shack in kit form. This particular aircraft was chosen for its large size and docile handling qualities. The aircraft is

*Major, USAF, Assistant Prof., Dept. of Aeronautics, USAFA.

configured for normal radio controlled operation to allow for initial testing, manual backup/override for safety, and manual takeoffs and landings. The aircraft is propeller powered by a 2.5 brake horsepower (BHP) two-stroke-cycle gasoline Quadra 35 engine. The aircraft (see Fig. 1) has a wingspan of 8.73 feet. The estimated weight with full fuel and computer on board is 30 pounds. The tricycle landing gear configuration, as shown in the picture, was later modified to conventional (tail wheel) for structural reasons and to facilitate operation on grass.

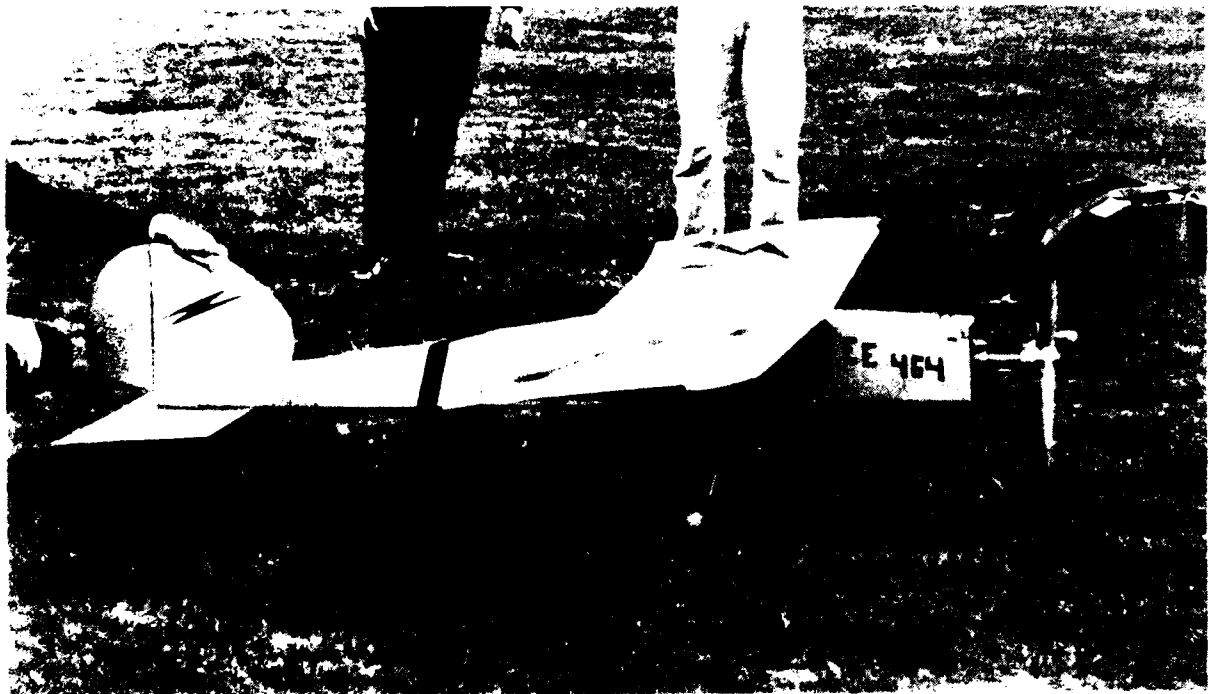


Figure 1. The Big Stick Airplane

The aircraft is controlled by conventional ailerons, rudder, elevator, and throttle. Drawings for the .122 scale wind tunnel model are contained in Appendix A.

III. The Control Problem

The purpose of the flight control system is to make the aircraft fly an arbitrarily specified (and not necessarily straight) path given continuous information on the current state of the aircraft through a limited number of sensors. The design of the flight control system was formulated as a multi-input multi-output feedback control problem. The actual parameters to be controlled were specified as altitude (h), airspeed (V), and heading (ψ).



Figure 2. The Control Problem

Referring to Figure 2, the control problem can be visualized as one of driving the values of h , V , and ψ to those of h_c , V_c , and ψ_c , respectively, where c denotes the commanded value.

The flight control system makes inputs to the aircraft by adjusting the settings or deflections of the elevator (δ_e), throttle (δ_T), ailerons (δ_a), and rudder (δ_r). These control settings depend on the sensor measurements, which contain information about the actual state of the aircraft, and the commanded values of altitude, airspeed, and heading. This process is depicted in Figure 3.

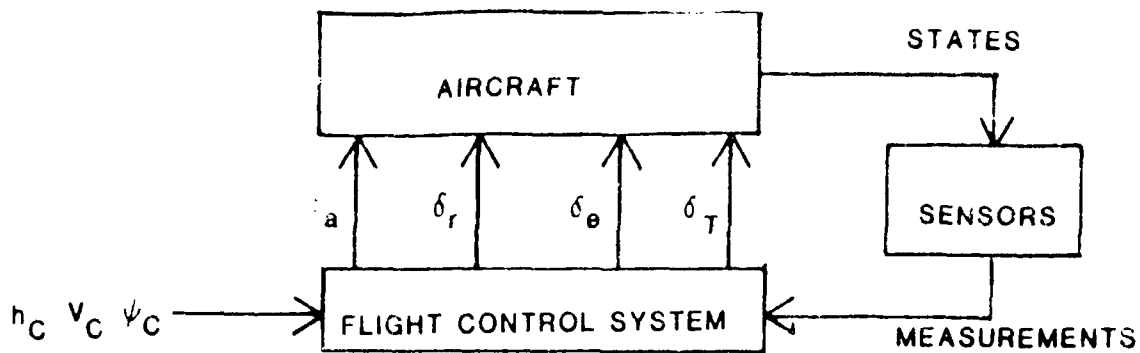


Figure 3. Control Process

The control system design problem, stated simply, was to find an algorithm to convert the commands and sensor measurements into the proper control settings to make the aircraft fly according to the commands.

Due to cost constraints, the sensors available for the project were limited to a yaw rate gyro, a lateral accelerometer, a heading indicator, an altimeter, and an airspeed meter. This is a very limited set of measurements considering the job required; therefore, it was feared that design of a satisfactory control system might prove impossible. For instance, note that there are no position gyros. This means that the control system is required to roll the aircraft in and out of turns with no feedback whatsoever as to the bank angle of the aircraft. Almost all three-axis autopilots in use today have position gyros for yaw, pitch, and roll angle measurements.

For design purposes, the measurements available to the flight control system were:

- n_y lateral load factor
- r yaw rate
- ψ heading

- h altitude
- V airspeed
- \dot{h} rate of climb (to be derived by numerically differentiating h)

IV. Design Procedure

"Classical" control theory methods (LaPlace transforms and root loci) were used in the design of this control system as opposed to "modern" optimal control techniques (although the state-space matrix representation was borrowed from modern theory).

Two important simplifications were made and carried throughout the entire design procedure. The first was that the control system was continuous instead of discrete. (Recall that the control system is to be implemented by a digital computer.) This assumption is not too unreasonable provided the cycle time of the computer is quite a bit faster than the aircraft response. The second simplification was that of perfect sensors. This means that the measurements of the aircraft's state provided to the control system are true and uncorrupted by noise. This simplification may or may not be valid, depending on the quality of the sensors. As is the case in many feedback control design problems, the sensors were of minor concern during the design process, but their performance will make or break the flight control system when it is implemented in the actual aircraft.

The design procedure consisted of four major steps:

1. Determining the control system structure
2. Formulating the complete system linear model
3. Selecting the control system gains
4. Checking the control system performance in a nonlinear simulation.

A. Control System Structure

The control system structure or framework was arrived at by paralleling the way a pilot flies an aircraft in instrument conditions without attitude information. (This type of flying is referred to as "needle, ball, and airspeed" flying and is normally only done as an emergency procedure following an attitude indicator failure.) The structure is shown in the block diagram in Figure 4.

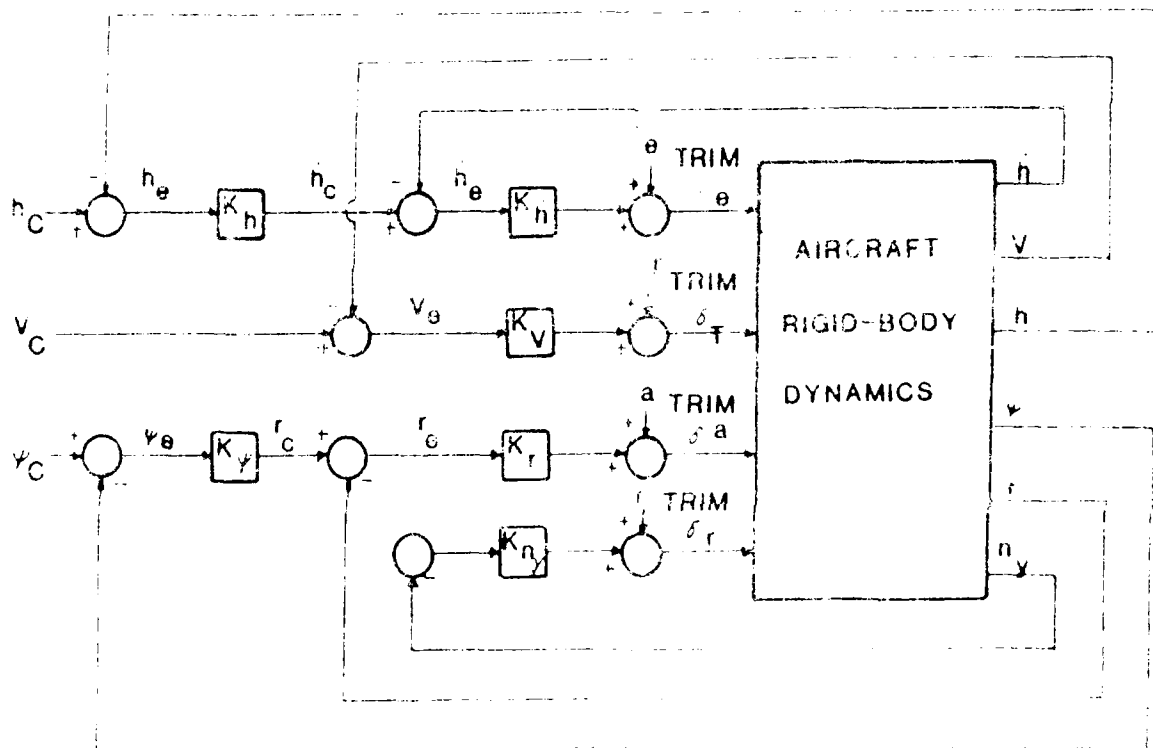


Figure 4. Flight Control System Structure (Basic)

In the block diagram (Figure 4), the square root block is there to convert the measured rate input signal by the constant, K , and Δ is the error signal. The circles represent summing that subtracts ψ_e and ψ_c from ψ . The subscript c denotes command values, e denotes error. The subscript r denotes rate, ψ denotes yaw angle, ψ_e denotes the error between the

commanded value and the actual value. The trim control values were added to allow the control system to operate relative to some reference steady-state condition and also to allow for compensation of items impossible to account for in the main model, such as wing warp, propeller torque, etc.

To see how the system works, let's look at the aileron (δ_a) control loop which is driven by heading (ψ). Suppose ψ_c is 015 degrees (0.262 rad.) but the actual heading, ψ , is 0 degrees or north. ψ_e then is 0.262 rad. This will result in a commanded yaw rate (r_c) of $\psi_e \times K_\psi$ rad/s. If the aircraft currently has zero yaw rate, r_e will also be $\psi_e \times K_\psi$ rad/s. From the diagram, δ_a will now be $r_e \times K_r$ more than $\delta_{a_{trim}}$. This will cause the aircraft to bank to the right and develop a positive yaw rate. As r approaches r_c , r_e gradually decreases and the aileron deflection is reduced. The aircraft is now turning. As ψ approaches ψ_c , r_c decreases and r_e goes negative. This deflects the ailerons in the opposite direction to gradually roll the aircraft out as ψ_c is approached. It is instructive to note that r is approximately equal to the rate of change of ψ . However, it is close for small bank angles. The same situation exists for the pilot flying heading, bank, and airspeed. Heading is usually controlled much more effectively through bank angle but that measurement is not available. Roll is controlled in exactly the same fashion. The rudder is used to control yaw rate directly, but it is not available to roll out any bank angle. The rudder is used in the same way by warping the wings to produce a roll moment. The rudder is also used to control yaw rate directly, but it is not available to roll out any bank angle. The rudder is used in the same way by warping the wings to produce a roll moment. The rudder is also used to control yaw rate directly, but it is not available to roll out any bank angle. The rudder is used in the same way by warping the wings to produce a roll moment.

wind tunnel testing conducted in the Air Force Academy's low speed wind tunnel by Cadet First Class Charles E. Myers and Daniel A. Draeger and by estimation methods contained in reference 5. The required mass data was obtained from Cadet First Class Thomas A. O'Berg through inertia testing of the actual aircraft. All of the aircraft data used are contained in Appendix B. The actual aircraft model is assembled in Appendix C.

The aircraft equations of motion were linearized about a steady-state condition of straight and level at 7500 feet, standard sea level airspeed of 73.33 ft/s (50mph). The usual two degree-of-freedom equations were obtained and are listed below:

$$\begin{bmatrix} \dot{u} \\ \dot{w} \\ \dot{p} \\ \dot{q} \end{bmatrix} = \begin{bmatrix} -0.014 & 0.000 & 0.000 & 0.000 \\ 0.000 & -0.000 & 0.000 & 0.000 \\ 0.000 & 0.000 & -0.000 & 0.000 \\ 0.000 & 0.000 & 0.000 & -0.000 \end{bmatrix} \begin{bmatrix} u \\ w \\ p \\ q \end{bmatrix} + \begin{bmatrix} 0.000 & 0.000 & 0.000 & 0.000 \\ 0.000 & 0.000 & 0.000 & 0.000 \\ 0.000 & 0.000 & 0.000 & 0.000 \\ 0.000 & 0.000 & 0.000 & 0.000 \end{bmatrix} \begin{bmatrix} \delta a \\ \delta e \\ \delta r \\ \delta \delta \end{bmatrix}$$

- δa = pitch angle change from steady-state in rad.
- δe = change in velocity component along longitudinal axis in ft/s
- δr = angle of attack change in rad.
- $\delta \delta$ = roll angle from steady-state in ft.
- $\delta \delta$ = roll rate from steady-state in rad/s.
- $\delta \delta$ = roll acceleration from steady-state in g's.

The aircraft model is assembled in Appendix C. The actual aircraft model is assembled in Appendix C.

1. The first of these is the

second of the three

third of the three

fourth of the three

the first of the three

the second of the three

the third of the three

the fourth of the three

the fifth of the three

the sixth of the three

the seventh of the three

the eighth of the three

the ninth of the three

the tenth of the three

(1)

the first of the three

the second of the three

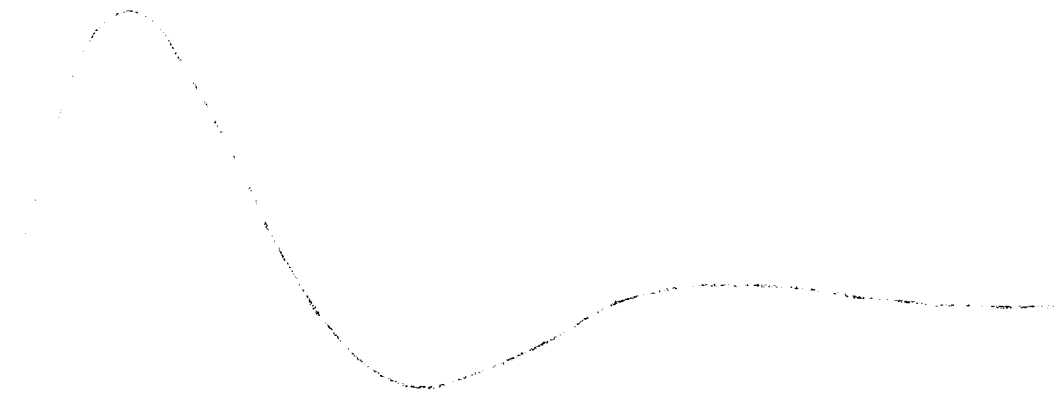
the third of the three



100
99
98
97
96
95
94
93
92
91
90
89
88
87
86
85
84
83
82
81
80
79
78
77
76
75
74
73
72
71
70
69
68
67
66
65
64
63
62
61
60
59
58
57
56
55
54
53
52
51
50
49
48
47
46
45
44
43
42
41
40
39
38
37
36
35
34
33
32
31
30
29
28
27
26
25
24
23
22
21
20
19
18
17
16
15
14
13
12
11
10
9
8
7
6
5
4
3
2
1
0

0 1 2 3 4 5 6 7 8 9 10 11 12 13 14 15 16 17 18 19 20 21 22 23 24 25 26 27 28 29 30 31 32 33 34 35 36 37 38 39 40 41 42 43 44 45 46 47 48 49 50 51 52 53 54 55 56 57 58 59 60 61 62 63 64 65 66 67 68 69 70 71 72 73 74 75 76 77 78 79 80 81 82 83 84 85 86 87 88 89 90 91 92 93 94 95 96 97 98 99 100

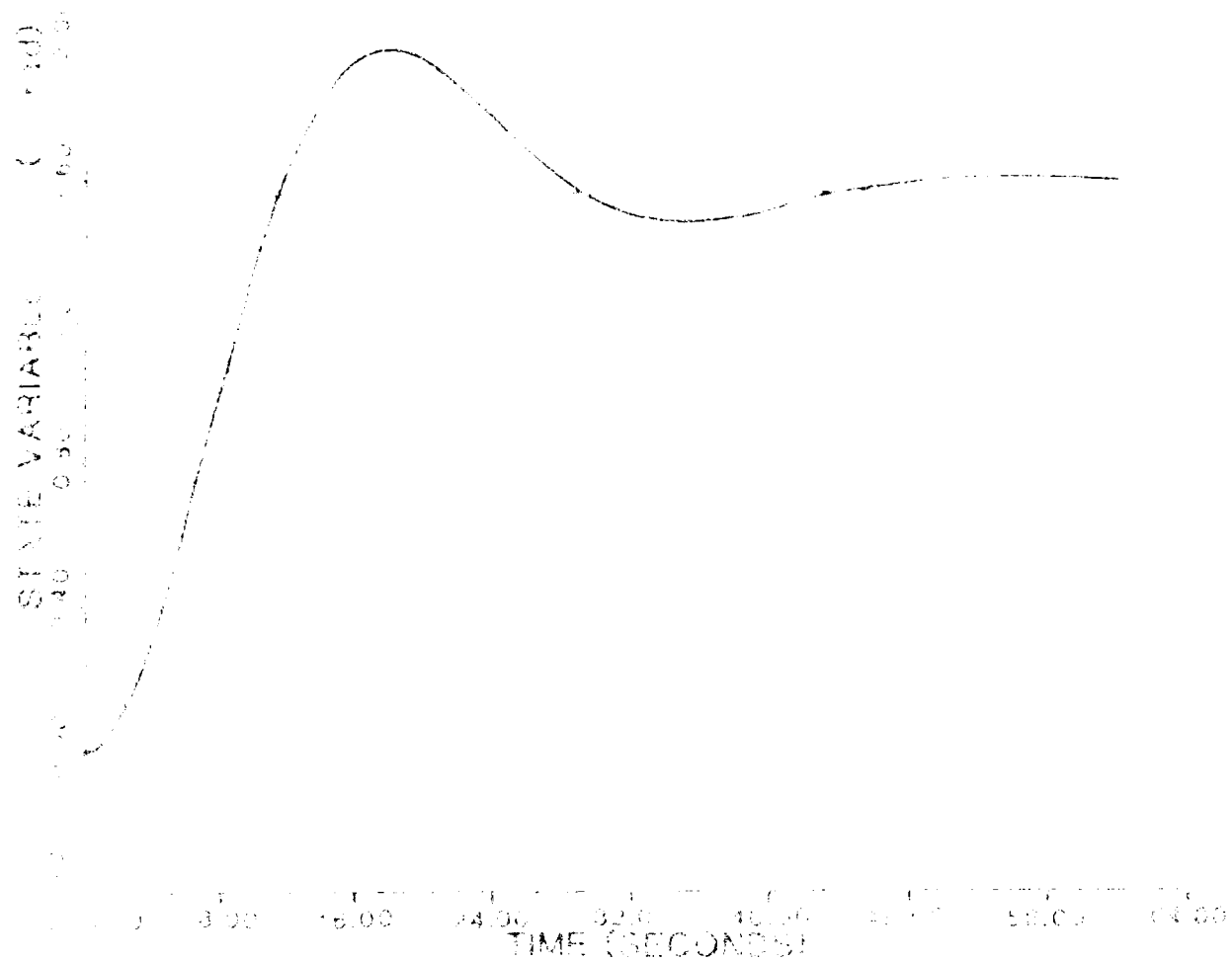
ALL VARIABLE 0.00 0.00 1.00



TIME (SECONDS)

FIGURE HISTORY

Figure History Simulation



FLIGHT HISTORY

1. Level 7 are Simulations

the wing stall. The results are shown in Figure 17. Figure 17 shows the heading again over the 15 second period. The heading value from Figure 18 we can see that the aircraft levels off at a value slightly below 7000 feet. Figure 19 shows that the velocity goes through some gyrations. It stabilizes at about 75 ft/s in the descent and then reduces to about 62 ft/s when the aircraft pulls out of the turn. Figure 20 is a plot of the throttle activity during this maneuver. It shows the throttle at idle from the 5 to 13 second point. The throttle then comes up to about 15% during the descent and then comes up to about 18 BH after the aircraft levels out.

B. Simulation

Simulations with the selected gains were run using the nonlinear simulation program of Appendix D. Limitations on control deflections and on some of the gains were added for reasons discussed in the last section. Four flight maneuvers were simulated. The initial conditions for each maneuver were the steady-state reference condition (straight and level with $\alpha=0$, $V=73.33$ ft/s, and $h=7500$ ft). The four maneuvers were:

- (1) level turn
- (2) straight climb
- (3) level, straight acceleration
- (4) combination turn, descent, and deceleration

1. Nonlinear Limits

The following control limits were used in the simulation based on estimated aircraft limits:

control	min.	max.
δ_a	-15 deg	15 deg
δ_T	0 BHP	2 BHP
δ_r	-15 deg	15 deg
$\delta_{\dot{h}}$	-15 deg	15 deg

Limits on commanded rate of climb (\dot{h}_c) were selected as ± 11.5 ft/s.

This corresponds to climb and descent angle of nine degrees. The

climb would require about 2 BHP at steady state. The commanded turn

rate limit was limited as ± 15 deg/s. This equates to a bank angle of ± 15 degrees and a turn radius of about 6,000 feet.

a. level turn simulation

A maneuver to a heading of 15 deg (1.92 rad) was required. The aircraft response is plotted in Figure 11.13. The

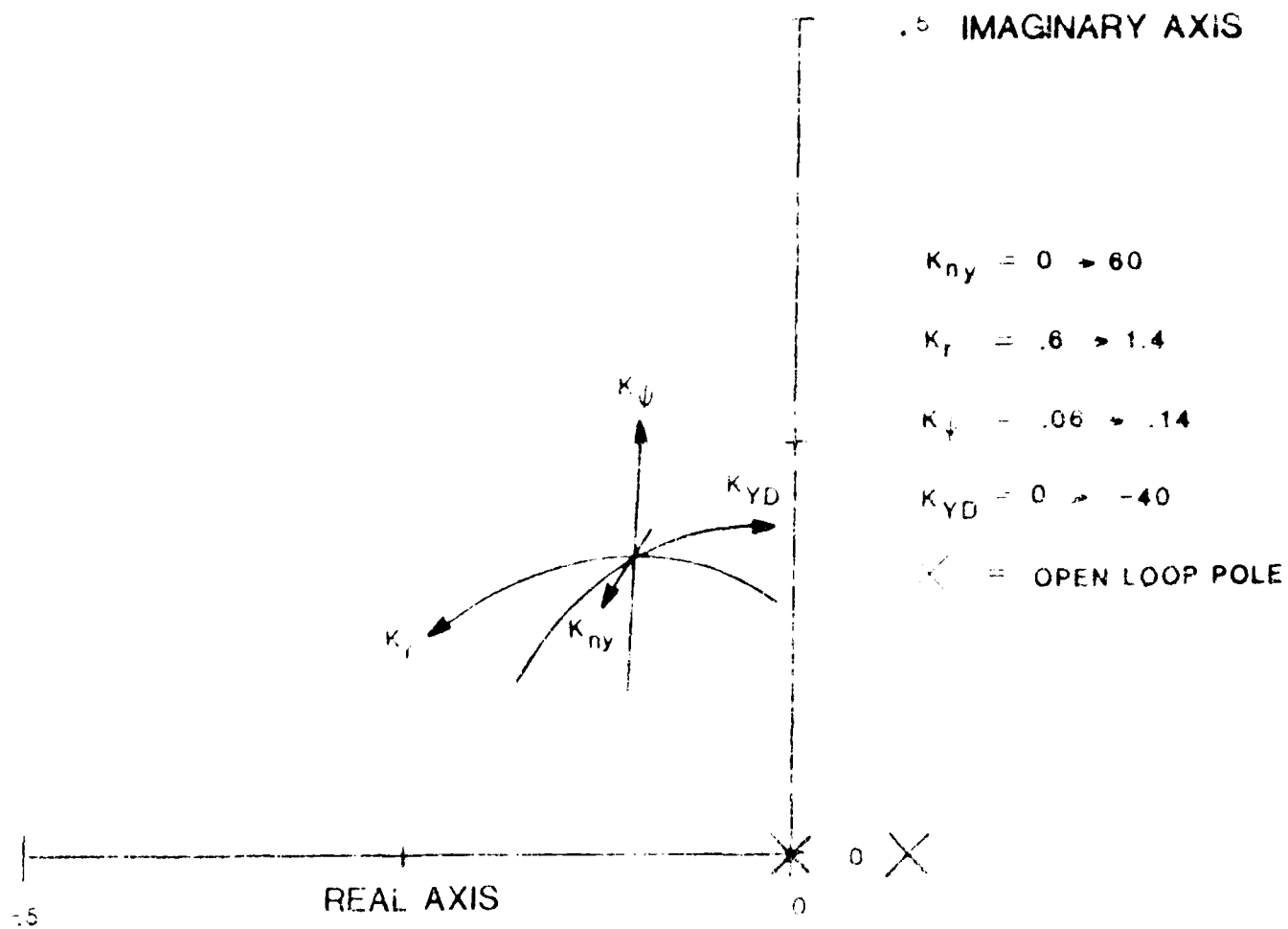


Figure 9. Lateral-Directional Root Loci (Blow-up)

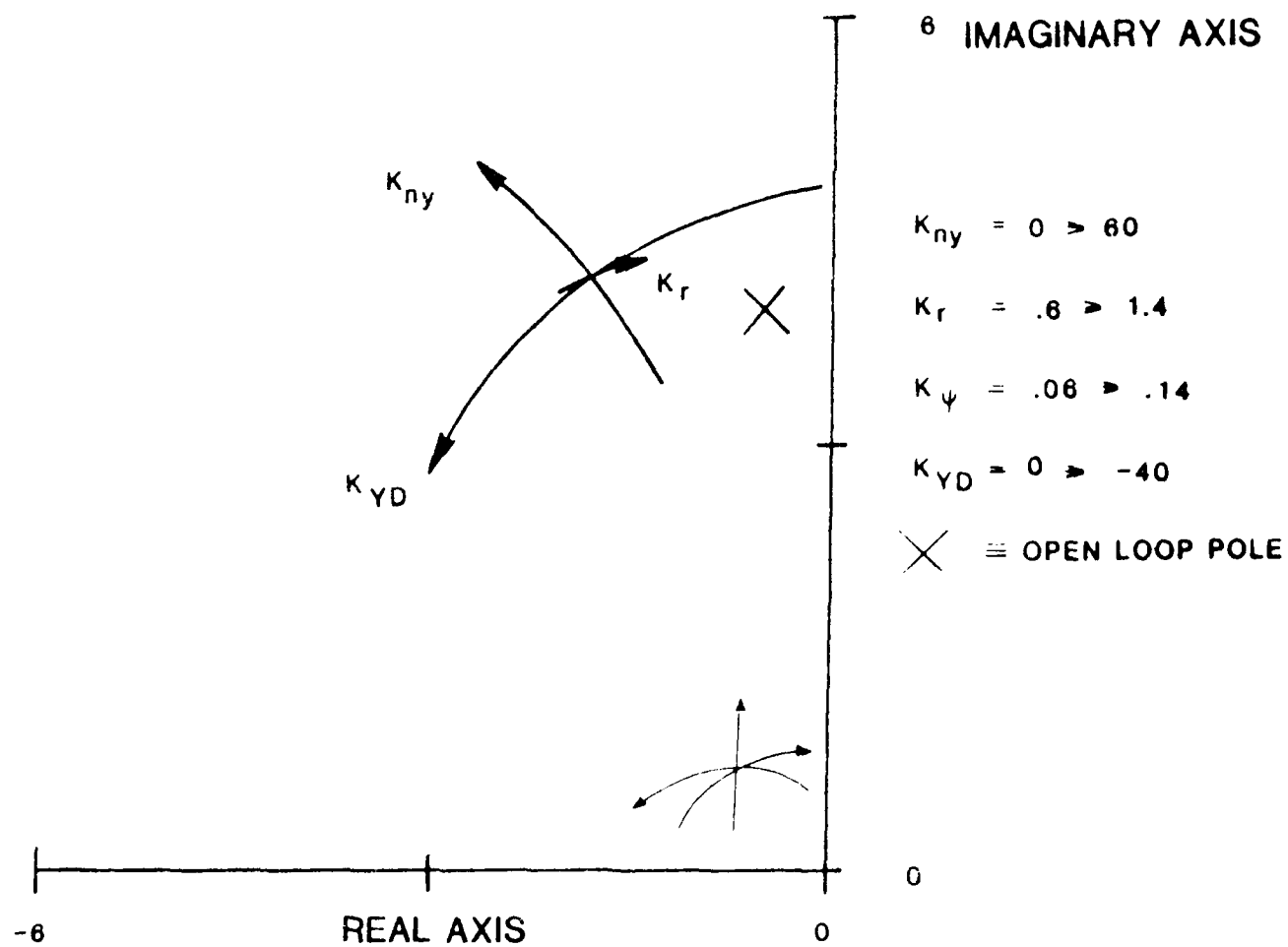


Figure 8. Lateral-Directional Root Loci

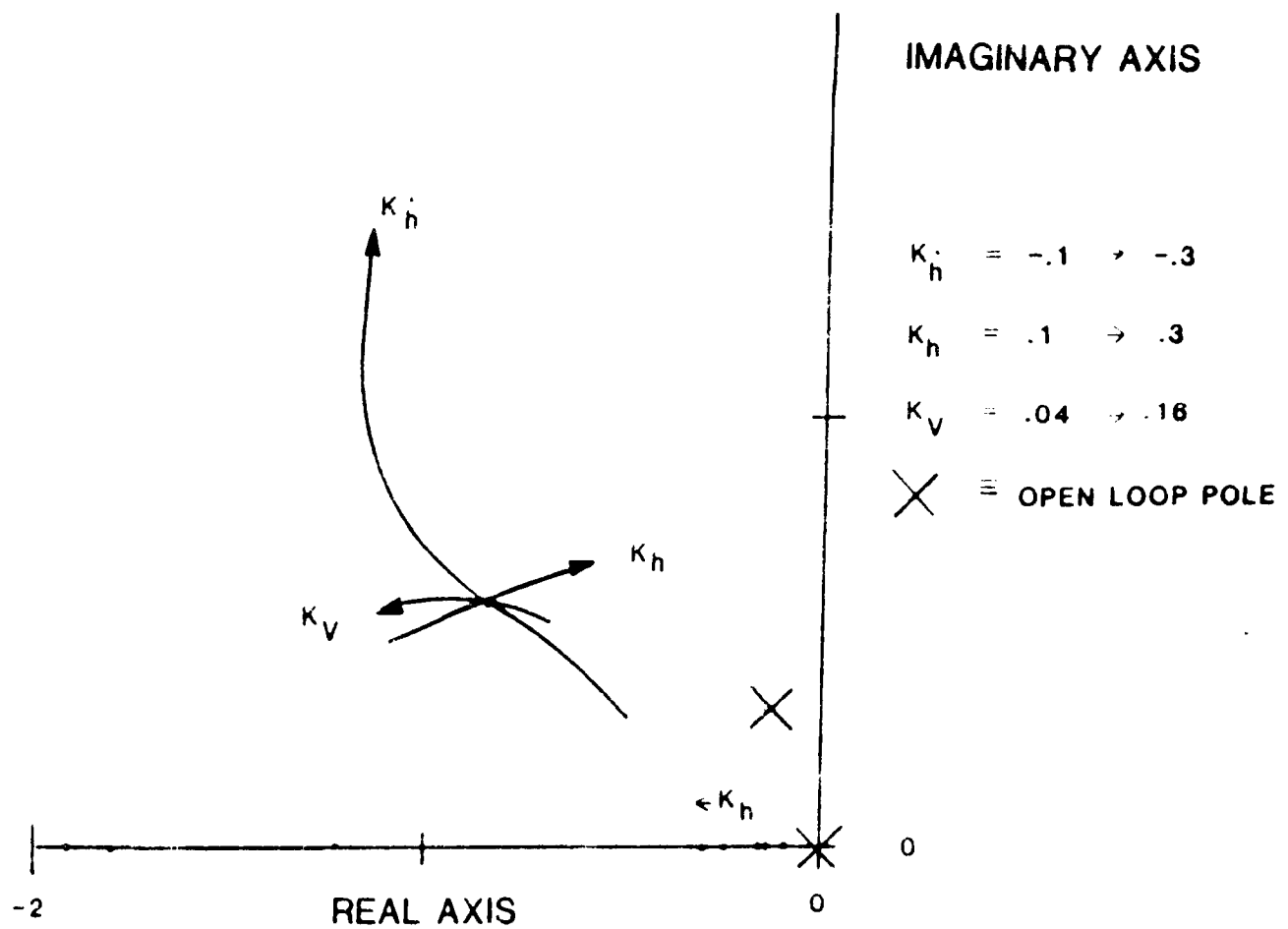


Figure 7. Longitudinal Root Loci

2. Lateral-directional case

The four lateral-directional gains selected were: $K_{ny} = 30$ deg/rad/sec, $K_r = 1$ rad/s/rad, and $K_{YD} = 20$ deg/rad/s. Figures 8 and 9 are the lateral-directional root loci plots. Figure 9 is a blow-up of the area around the origin in Figure 8. Again, a computer printout of the poles for each set of gains plotted is

tabulated in Appendix L.

The simulation results for the selected gains are presented in the next section.

V. Results

A. Root Loci

In multi-loop feedback systems, such as the one being dealt with in this report, the gains affect the system poles in an interrelated and complex fashion. A "shotgun" (trial and error) approach was used to initially find a neighborhood of gains that appeared to give reasonable poles. The gains were then varied in a more systematic fashion to refine the gain selection. Gains were selected on the basis of the speed and stability of the resulting poles. This was done separately for the longitudinal and lateral-directional cases.

1. Longitudinal case

The three longitudinal gains selected were:

$K_{\theta} = -.2 \text{ deg/ft/s}$, $K_h = .2 \text{ ft/s/ft}$, and $K_V = .1 \text{ BHP/ft/s}$. Figure 7 shows a segment of the longitudinal root loci plot that indicates how the poles are affected by the gains around the selected values. Only the upper left quadrant of the complex plane is shown since any values in the right half plane are unstable and unacceptable and since the bottom half plane is a mirror image of the top. The actual values of the poles plotted are contained in the computer printout in Appendix E.

gains.

The root loci were constructed by varying the gains and solving for the poles after each change. This process had to be computerized. Separate programs were written on an Apple microcomputer for the longitudinal and lateral-directional cases. The results are discussed in the next section.

D. Nonlinear Simulation

A 12 degree of freedom nonlinear Big Stick simulation program was written for the Burroughs 6900 computer at the Air Force Academy by Cadet First Class Daniel A. Draeger. A hard copy is included in Appendix D. This simulation provides a much more accurate mathematical model of the aircraft than the linearized equations which were used to determine the control gains. Basically, the program numerically integrates the nonlinear aircraft equations of motion from Reference 1, modified to include the control system, and plots out any of the state variables versus time. The nonlinear equations do not decouple into longitudinal and lateral-directional sets.

The simulation was run to see how the control gains, selected under the linear assumption, would actually perform in the real, nonlinear world. The effects of such elements as control deflection limits and changes in air density could be observed. The simulation was also used to check the limiting values for r_c and \dot{h}_c . These are cutoff values which had to be incorporated into K_h and $K_{\dot{h}}$ to prevent the aircraft from stalling itself out or entering a steep dive in the case of a big change in h_c or rolling inverted when r_c changed. A side benefit of the simulation is that it provides a check on the previous calculations. Performance should be close to the linear prediction around the steady-state condition.

pole indicates the stability of its associated mode (- for stable, + for unstable, 0 for neutral) and the imaginary part indicates the oscillation frequency (aperiodic if real). Complex poles occur in conjugate pairs. The magnitude of the pole (distance from origin) indicates the speed of the associated mode. For example, in Figure 6, poles 1, 2, and 5 are aperiodic. Poles 1 and 5 are stable while 2 is unstable. The mode associated with pole 5 will die out faster than the one associated with pole 1. The complex conjugate pairs 3 and 4 represent oscillatory modes. Mode 3 is stable and 4 is unstable.

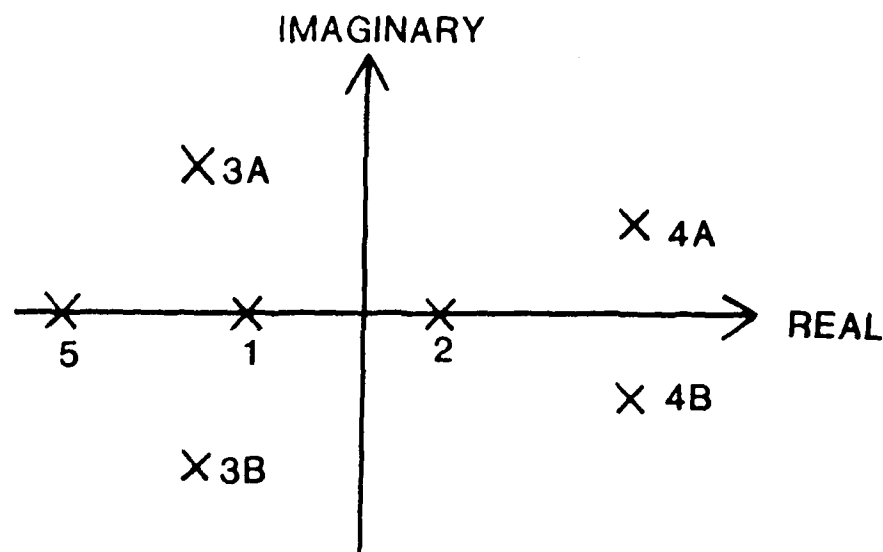


Figure 6. Poles on the Complex Plane

It can be shown (Ref. 4) that the characteristic equation of a system described by Equation 3 is $\det(\lambda[I] - [A]) = 0$ where λ is an arbitrary scalar number and $[I]$ is an identity matrix. The solutions of the equation for λ are the poles. We are interested in the poles of the closed-loop system, Equation 10. These can be determined by solving $\det(\lambda[I] - [A-BF]) = 0$. The F matrix, of course, depends on the

For the lateral-directional model:

$$[F] = \begin{bmatrix} 0 & 0 & K_r & 0 & K_\psi K_r \\ 1.22K_{ny} & .000634K_{ny} & K_{YD} - .0285K_{ny} & 0 & 0 \\ 1 - .00624K_{ny} & 1 - .00624K_{ny} & 1 - .00624K_{ny} & 0 & 0 \end{bmatrix} \quad (7)$$

$$[B'] = \begin{bmatrix} K_\psi K_r & 0 \\ 0 & 0 \end{bmatrix} \quad (8)$$

By substituting (4) into (3), we obtain

$$\dot{\bar{x}} = [A] \bar{x} + [B] \{-[F] \bar{x} + [B'] \bar{u}_c\}. \quad (9)$$

Combining terms gives

$$\dot{\bar{x}} = [A - BF] \bar{x} + [BB'] \bar{u}_c \quad (10)$$

The complete linearized system model (or closed-loop system), then, consists of two independent equations of the form of Equation 10 -- one for longitudinal motion and one for lateral-directional motion. The vectors and constant matrices have been defined for each case.

C. Determination of Control System Gains

The core of the feedback control problem is the selection of the control gains. In this project, that means finding values of K_h , K_ψ , K_V , K_r , K_{ny} , and K_{YD} that give satisfactory response to aircraft heading, altitude, and airspeed commands in the presence of disturbances such as wind gusts.

The response of any linear dynamic system is characterized by the roots of its characteristic equation (also called system poles or eigenvalues). Root loci were used in this project to select the gains. A root locus is a complex plane plot showing how a pole varies as a gain is changed. By way of review, the sign of the real part of the

algebraic combinations of the states. Equation 1 shows that this is true for the measurement \dot{h} . This is also true for n_y^1 . V is closely approximated by u . It is possible, then, in both the longitudinal and lateral-directional cases to express the controls as:

$$\bar{u} = - [F] \bar{x} + [B'] \bar{u}_c \quad (4)$$

where $[F]$ is called the feedback matrix and $[B']$ is called the input matrix. The vector \bar{u}_c is the command which is defined as $[h_c, V_c]^T$ for the longitudinal case and $[\psi_c, 0]^T$ for the lateral-directional case.

From Figure 5 and Equation 1 and 2 the feedback and input matrices were determined to be as follows:

For the longitudinal model:

$$[F] = \begin{bmatrix} 0 & 73.33K_h^* & 0 & -73.33K_h^* & K_h K_h^* \\ 0 & 0 & K_v & 0 & 0 \end{bmatrix} \quad (5)$$

$$[B'] = \begin{bmatrix} K_h K_h^* & 0 \\ 0 & K_v \end{bmatrix} \quad (6)$$

¹ n_y is lateral load factor which is equal and opposite to nongravitational lateral acceleration, normalized to the acceleration of gravity, g . It can be shown from Reference 1 and Appendix C that for the linearized approximation, $n_y = 1.222\beta + .000634p - .0285 r - .00624\delta_r$, which is a linear, algebraic combination of the states. (δ_r is a combination of the states only, since there are no commands that feed into the rudder.)

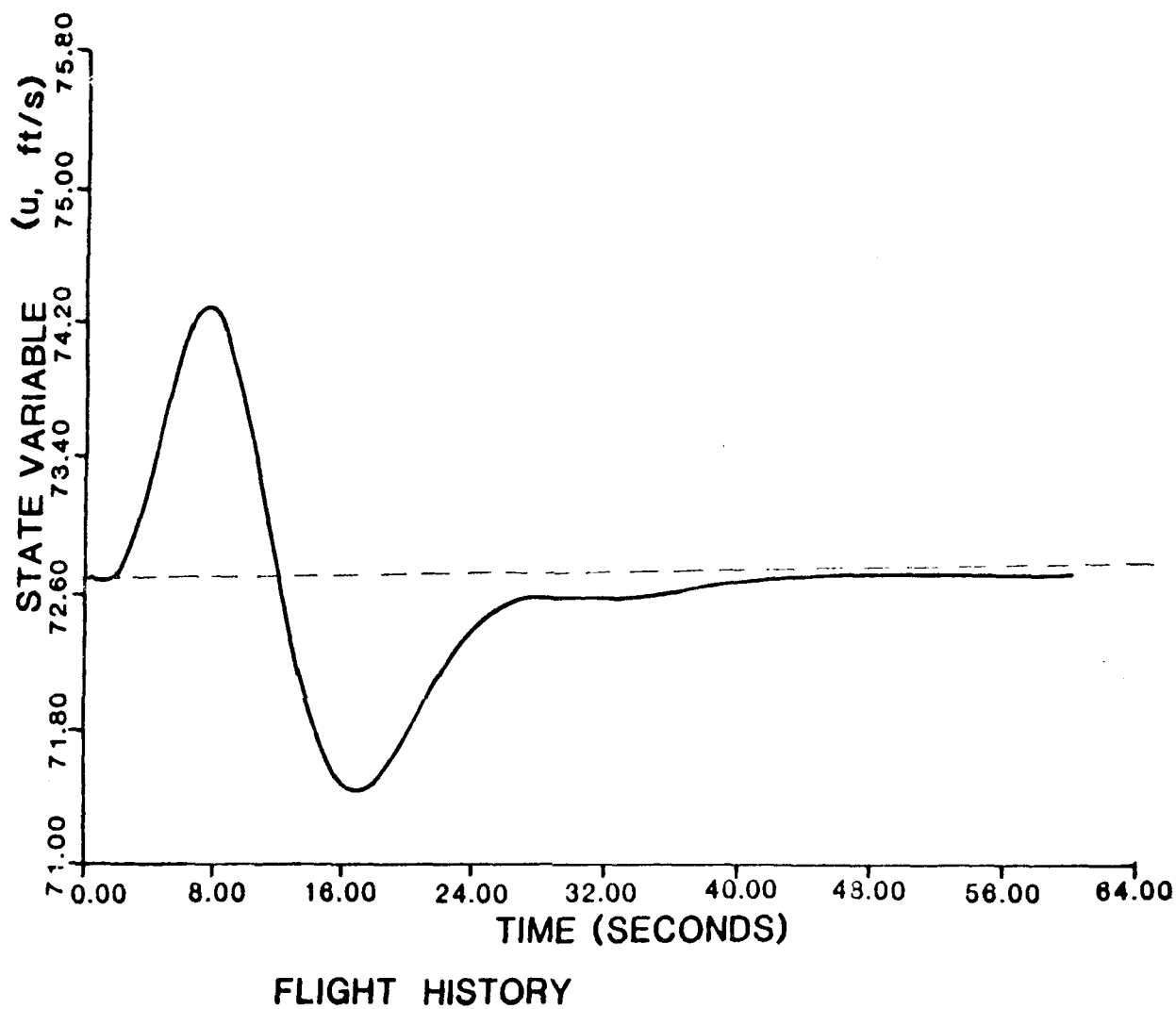
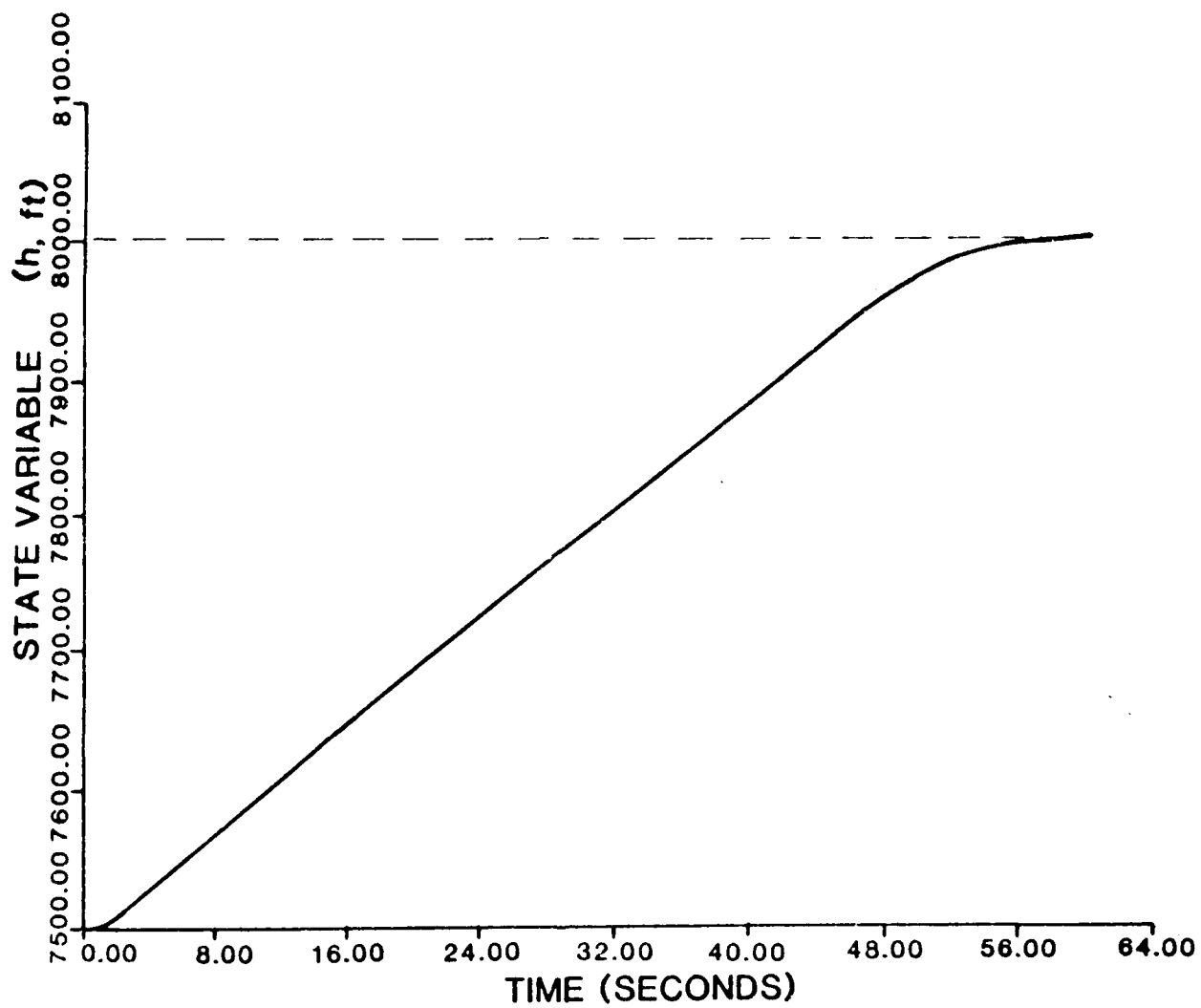
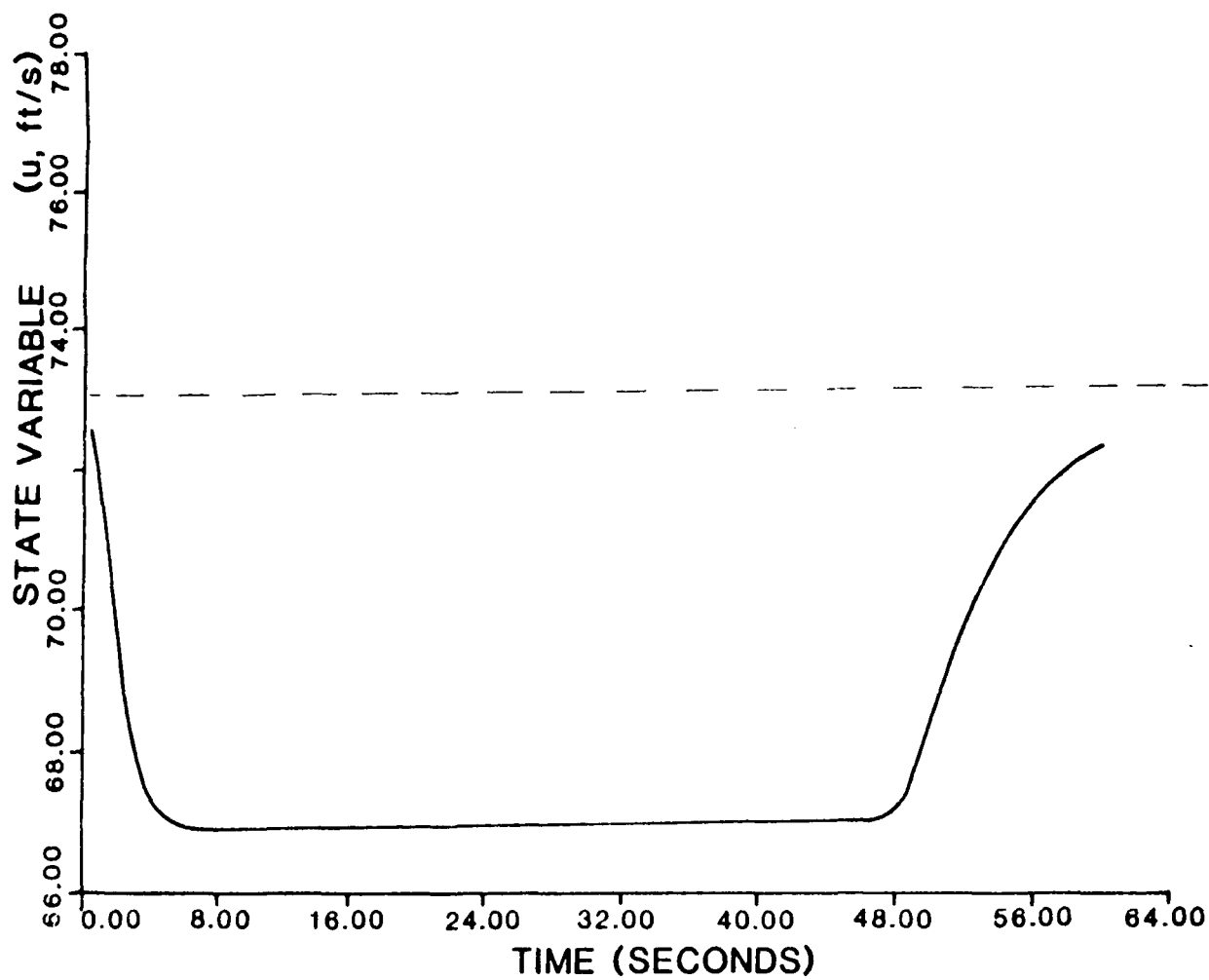


Figure 13. Level Turn Simulation - u



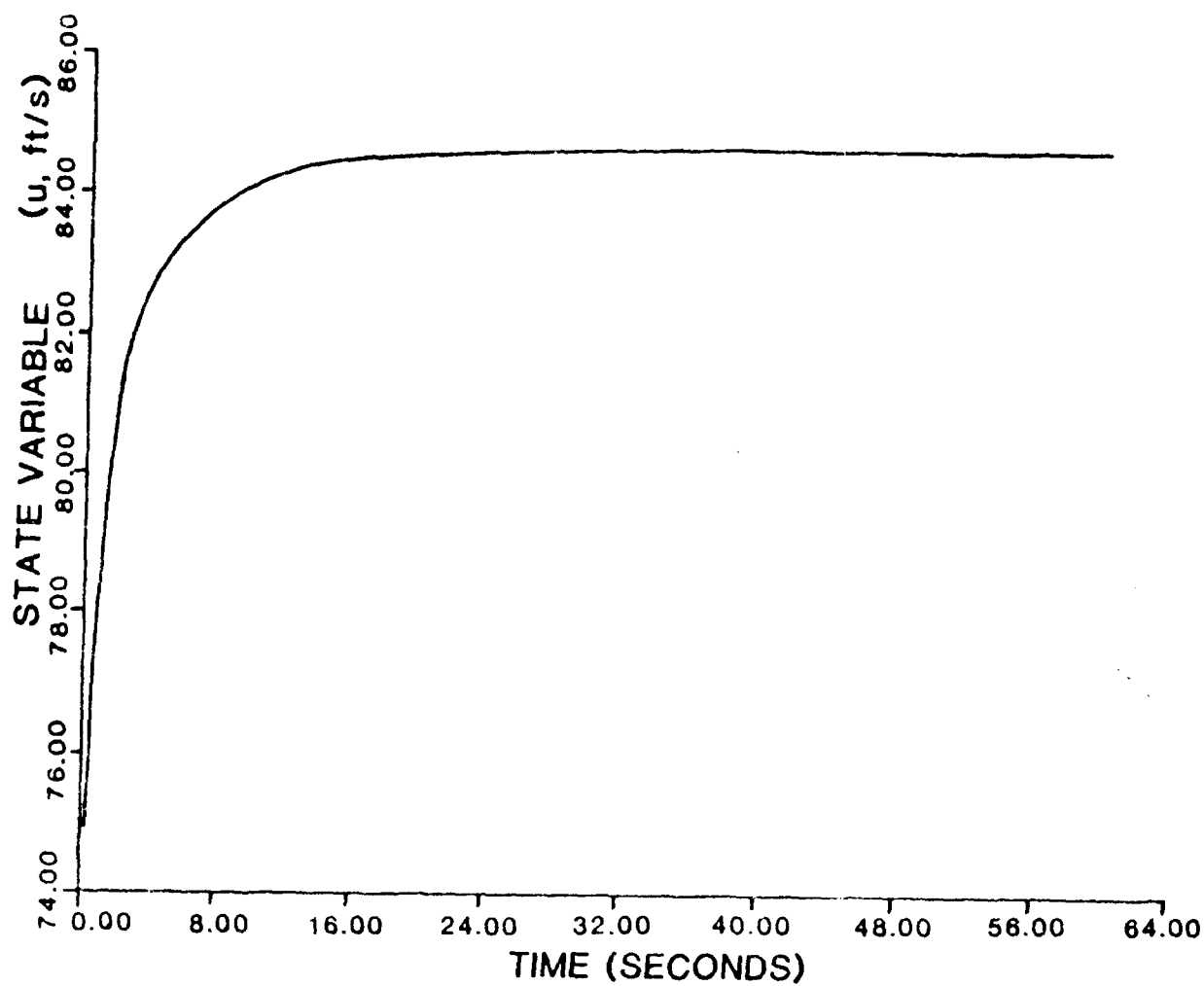
FLIGHT HISTORY

Figure 14. Straight Climb - h



FLIGHT HISTORY

Figure 15. Straight Climb Simulation - u



FLIGHT HISTORY

Figure 16. Level Acceleration Simulation - u

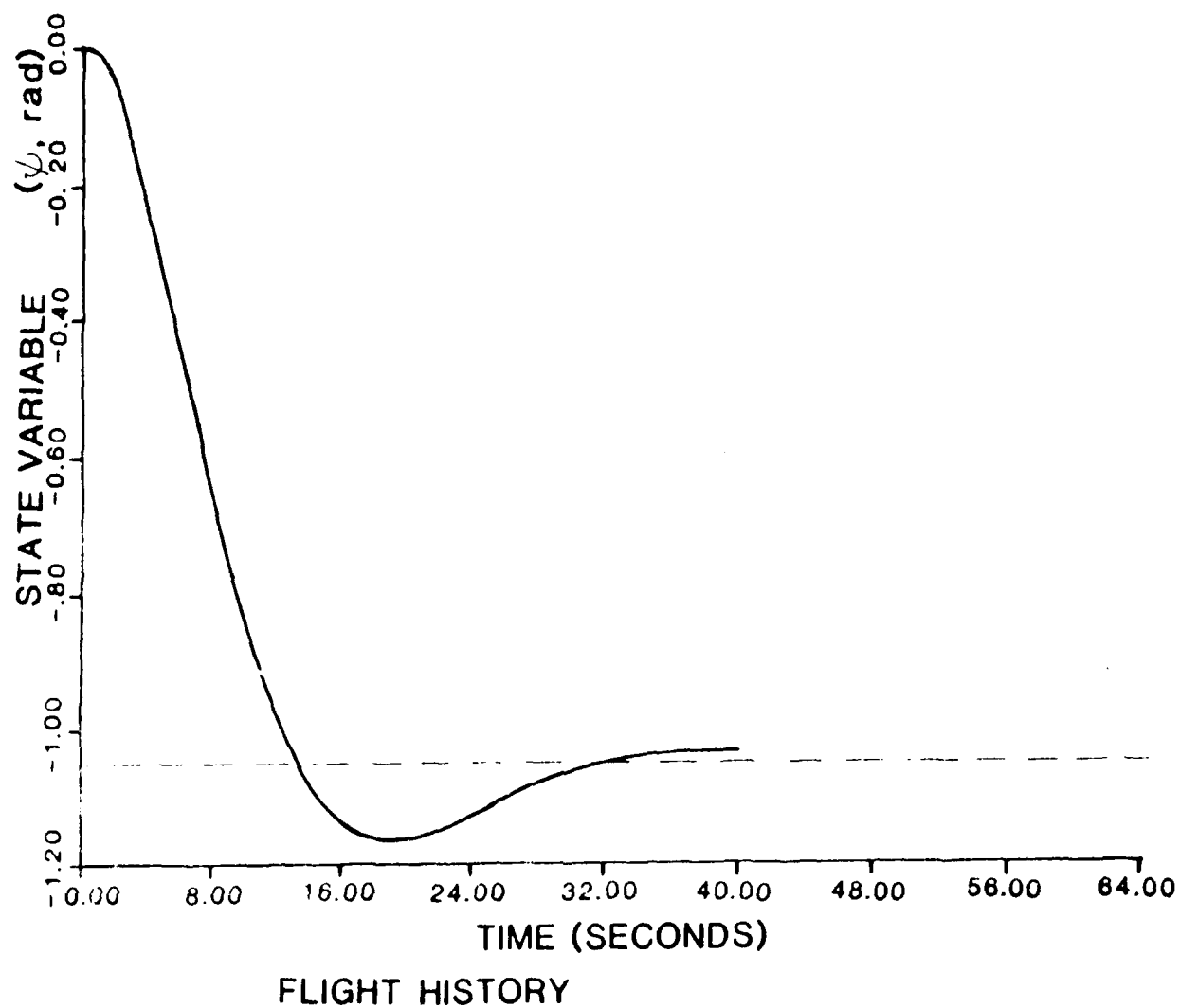
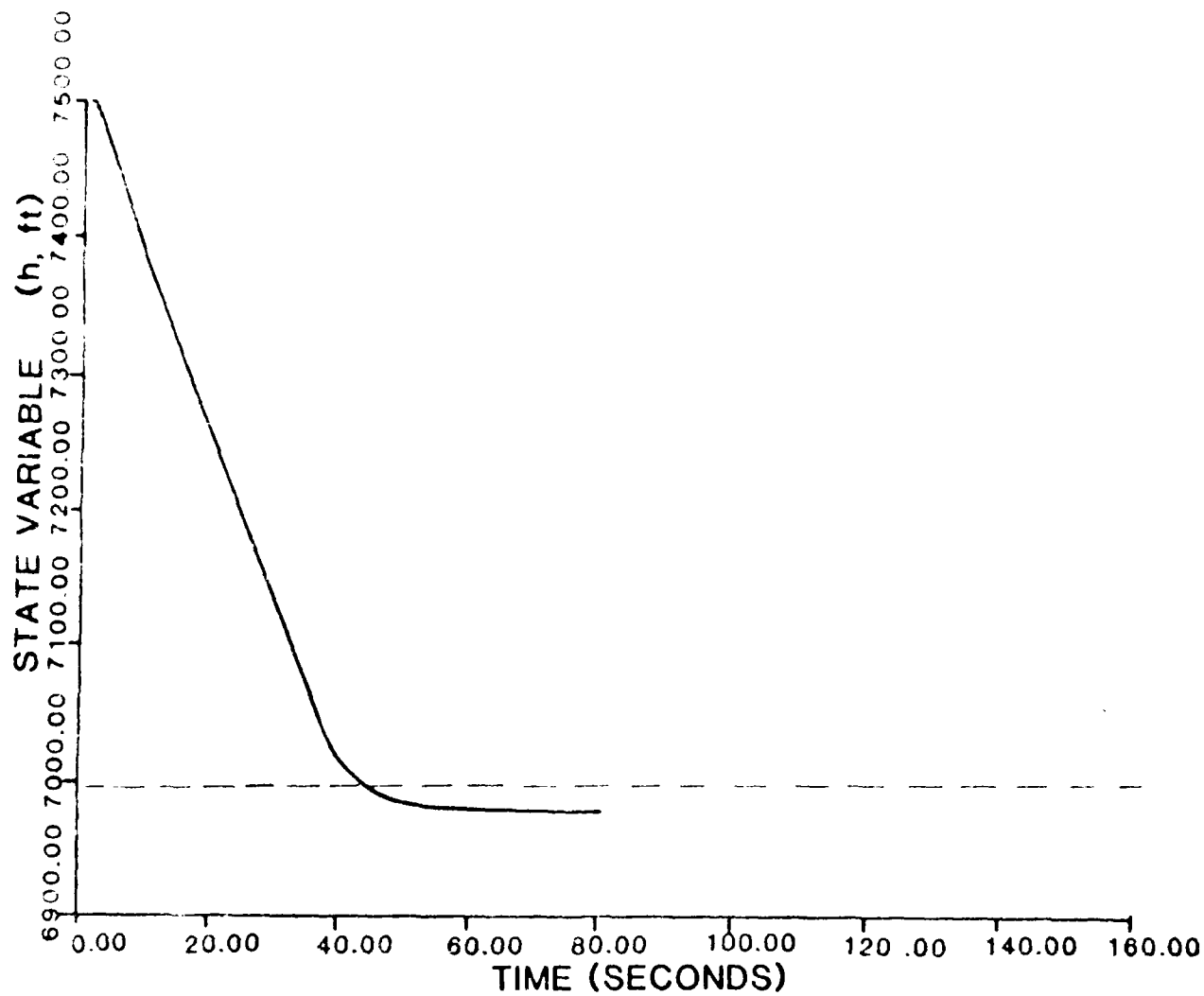
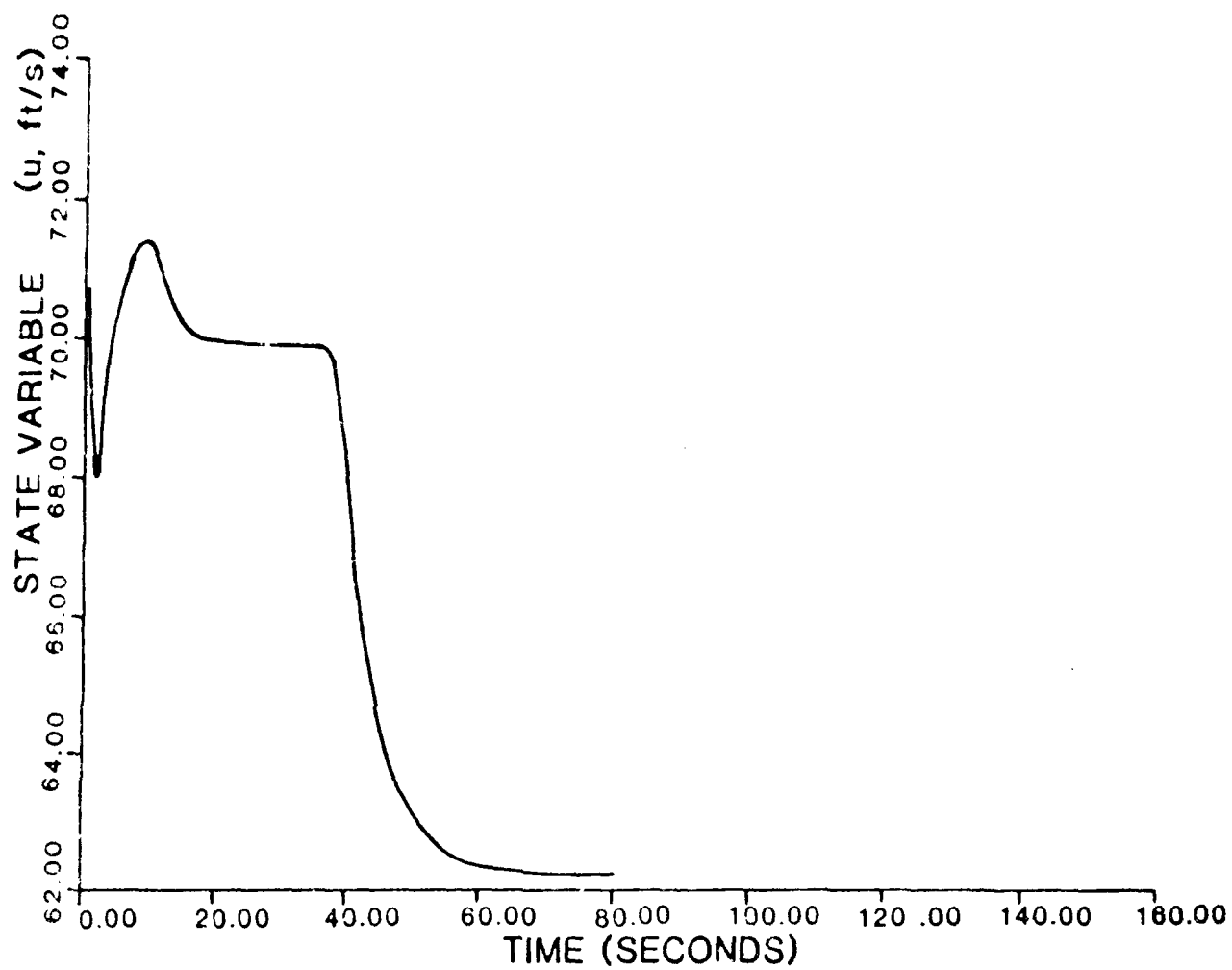


Figure 17. Multi-command Simulation - ψ



FLIGHT HISTORY

Figure 18. Multi-command Simulation - h



FLIGHT HISTORY

Figure 19. Multi-command Simulation - u

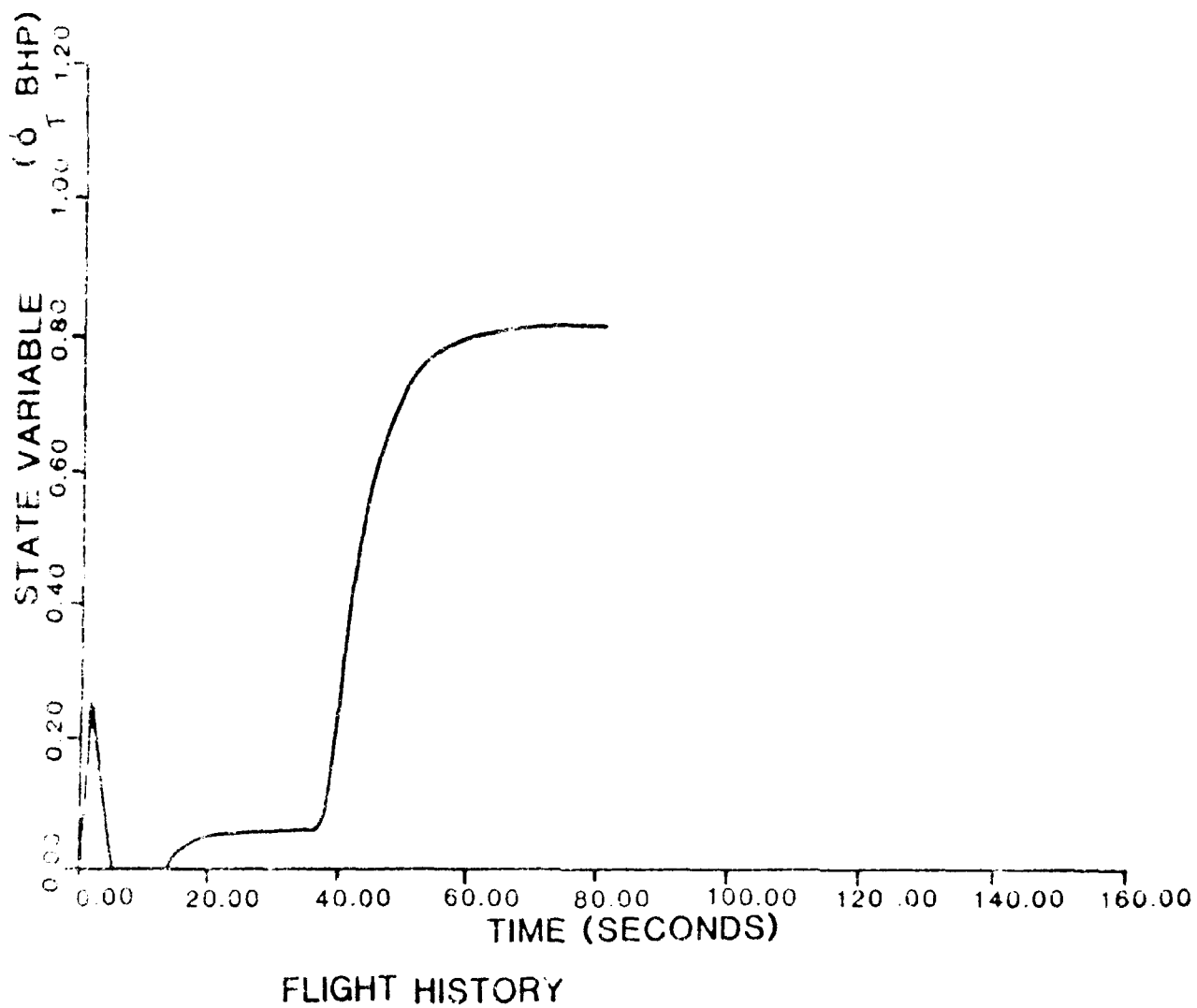


Figure 20. Multi-command Simulation - δ_1

VI. Recommendations

Based on the previous analysis, the following recommendations are made for the Big Stick flight control system:

1. That the control structure of Figure 5 be used.
2. That the following control gains be used:

$$K_{\dot{h}} = 1.2 \text{ (ft/s)/ft}$$

$$K_{\dot{h}} = -1.2 \text{ deg/(ft/s)}$$

$$K_V = 1.1 \text{ BHP/(ft/s)}$$

$$K_{\dot{\gamma}} = 1 \text{ (rad/s)/rad}$$

$$K_{\dot{\gamma}} = 1 \text{ deg/(rad/s)}$$

$$K_{\dot{\gamma}} = 30 \text{ deg/g}$$

$$K_{YD} = -20 \text{ deg/(rad/s)}$$

3. That \dot{h}_C be limited to ± 11.5 ft/s and $\dot{\gamma}_C$ be limited to ± 12 rad/s.
4. That a washout filter be included in the yaw damper feedback loop to pass the dutch roll frequency (4 rad/s) and attenuate the steady-state commanded yaw rate.
5. That the trim control settings be determined from flight test at the steady-state flight condition of straight and level at 73.33 ft/s and 7500 feet.

In implementing the flight control system, the same sign conventions must, of course, be used as are used in the aircraft equations of motion. These are (from Appendices C and D and Reference 1):

1. Positive for trailing edge down

2. Positive for trailing edge left

3. Positive for right up and left down $\dot{\gamma} = (\dot{\alpha}_L - \dot{\alpha}_R)/2$

4. Positive to right

1. Introduction

2. Background

3. Literature

1. J. H. Davenport, "The Dynamics of Shipboard Motion," *Journal of Ship Research*, Vol. 1, No. 1, 1957, pp. 1-10.

2. J. H. Davenport, "The Dynamics of Shipboard Motion," *Journal of Ship Research*, Vol. 1, No. 1, 1957, pp. 1-10.

3. J. H. Davenport, "The Dynamics of Shipboard Motion," *Journal of Ship Research*, Vol. 1, No. 1, 1957, pp. 1-10.

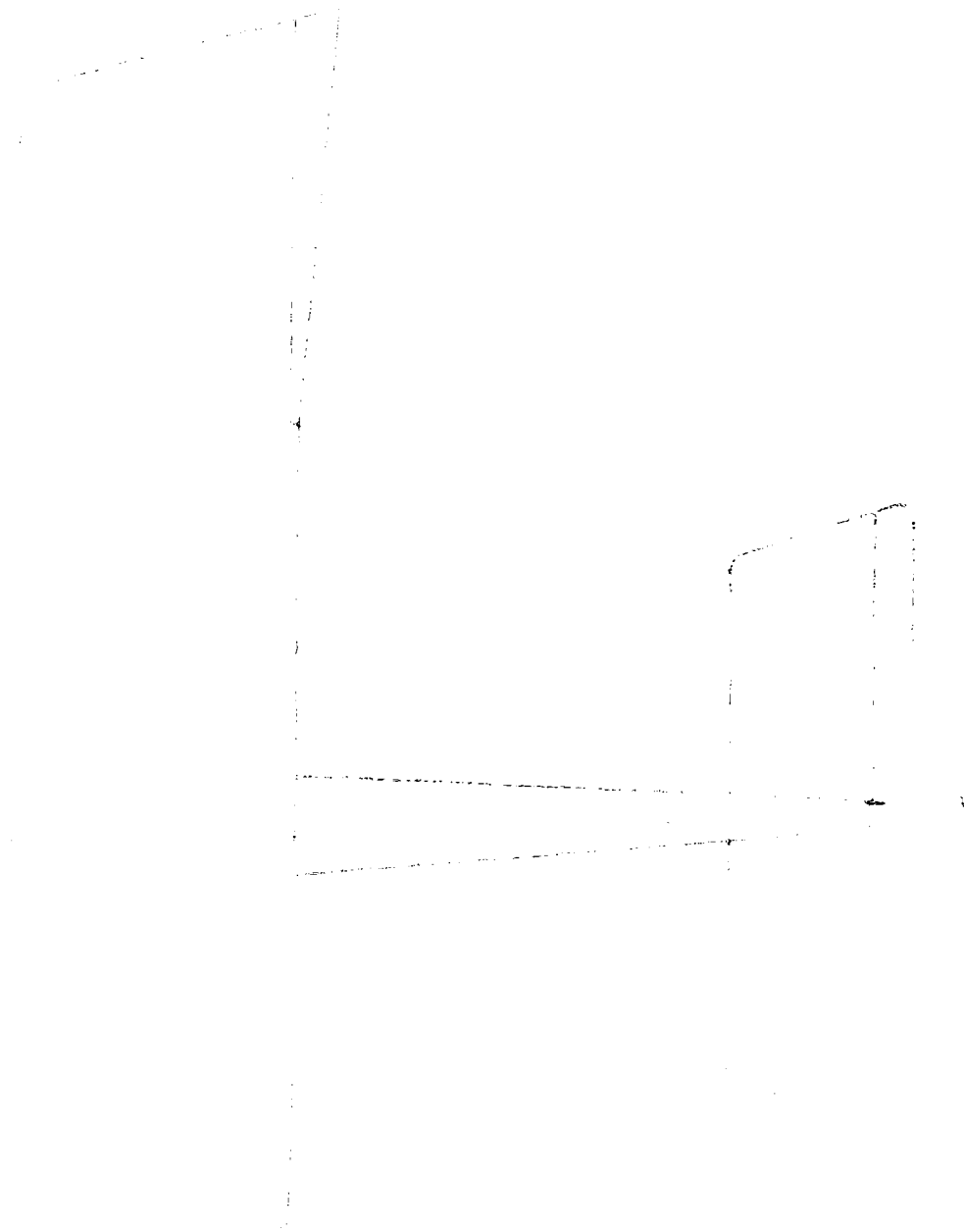
4. J. H. Davenport, "The Dynamics of Shipboard Motion," *Journal of Ship Research*, Vol. 1, No. 1, 1957, pp. 1-10.

5. J. H. Davenport, "The Dynamics of Shipboard Motion," *Journal of Ship Research*, Vol. 1, No. 1, 1957, pp. 1-10.

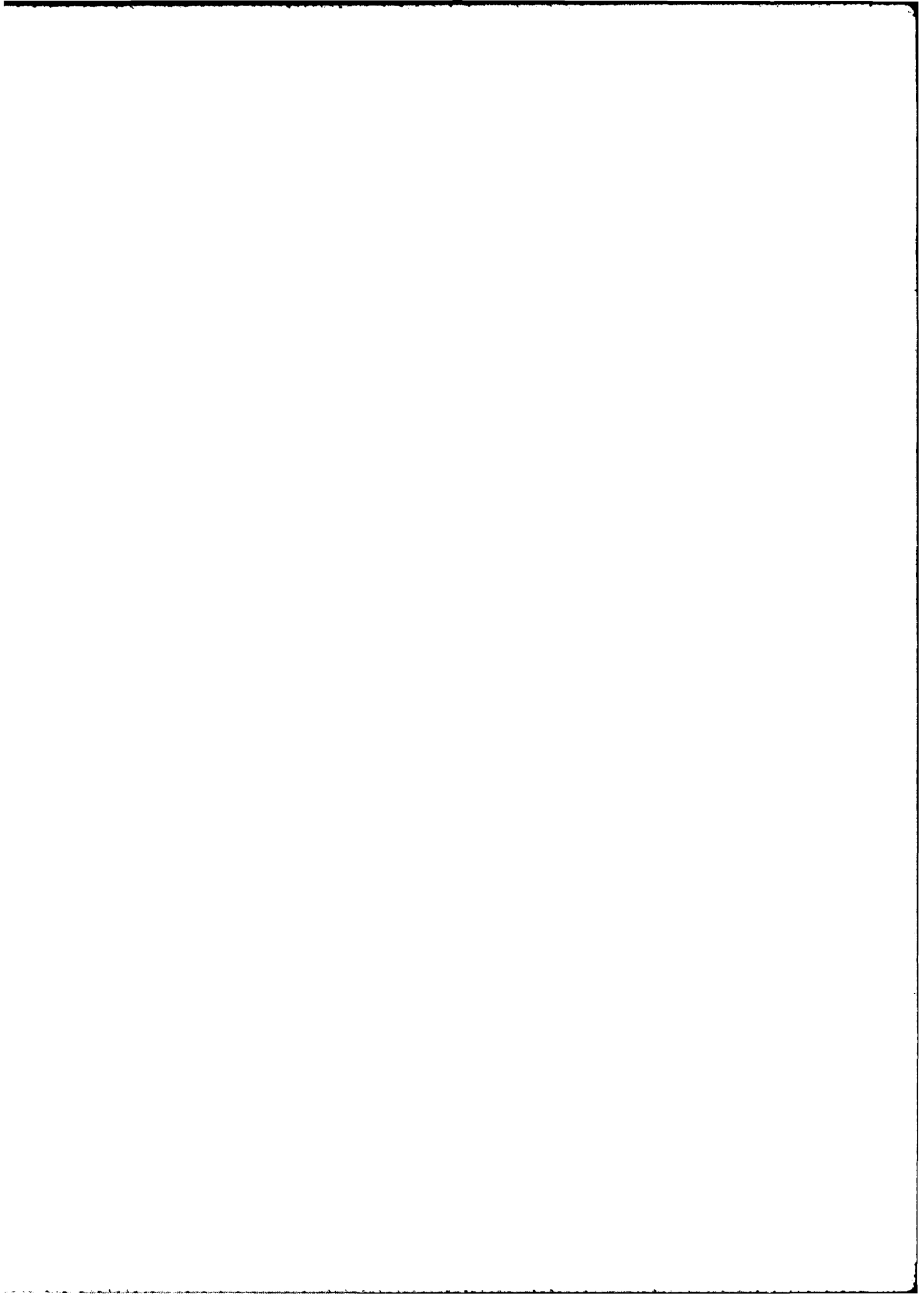
APPENDICES

10-1-77

APPENDIX A - 100 SCALE AND 1000 SCALE DRAWINGS

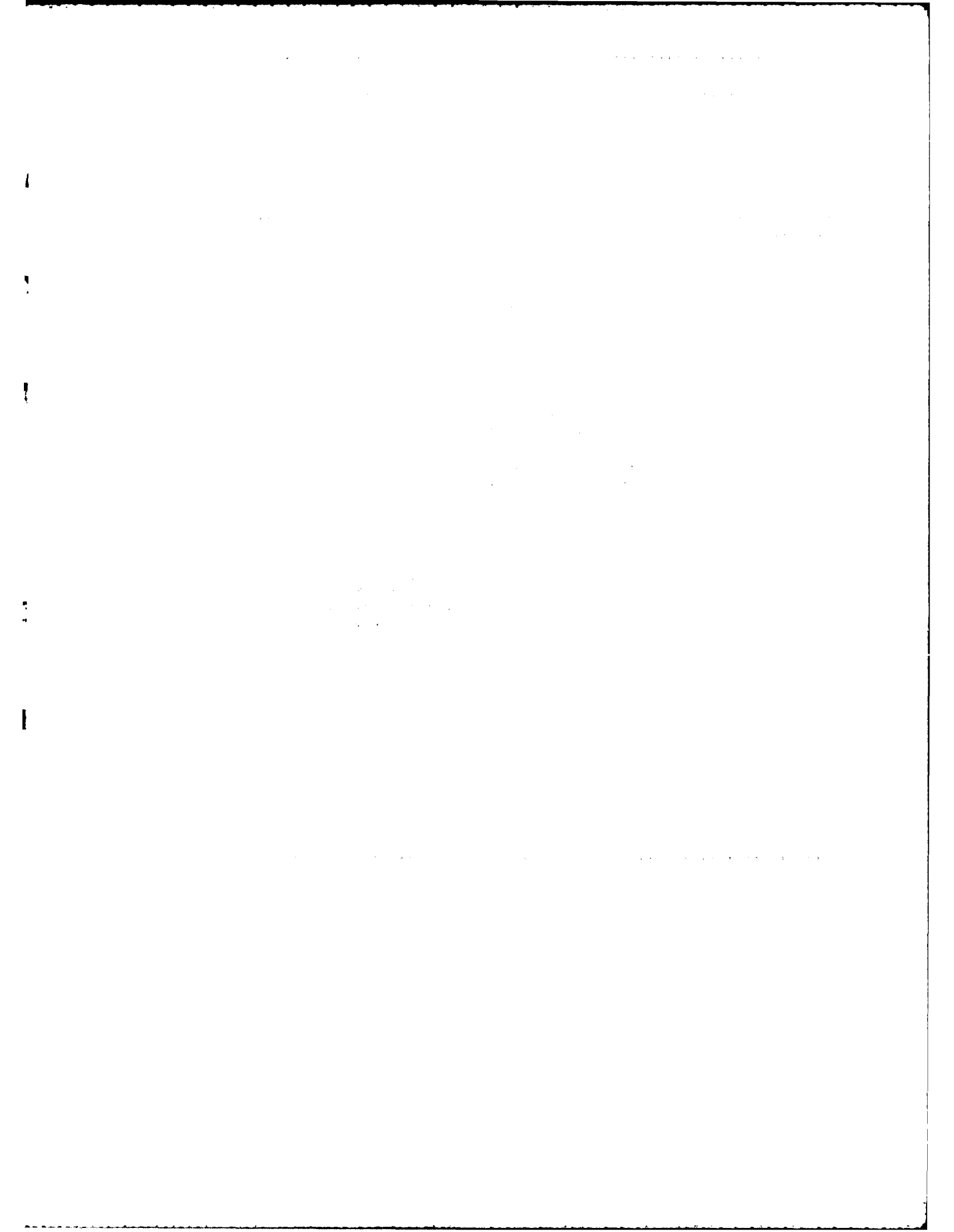












[illegible]

[illegible]

===== File - DSNUMINT =====

```

100 #RESET FREE
200 FILE 4 TITLE="CONSTN.",KIND="DISK",FILETYPE=7)
300 FILE 5 TITLE="SYSDAT.",KIND="DISK",FILETYPE=7)
400 FILE 6 (KIND="PRINTER")
500 FILE 7 (KIND="REMOTE")
600 FILE 8 (KIND="REMOTE")
700 #INCLUDE "PLOT/INCLUDE/FORTRAN."
800 #INCLUDE "(AERO457) DEAN/PLOTTER"
800 C *****
900 C ***FOLLOWING IS A LIST OF VARIABLE NAMES AND USES IN MAIN PROGRAM***
1000 C          DT = STEP SIZE IN NUMERICAL INTEGRATION
1100 C          T = TIME THE INTEGRATION IS CURRENTLY AT
1110 C          X = STATE VAR. ARRAY- U,V,W,F,C,R,PSI,THE,PHI,N,E,H
1120 C          DX = DERIVATIVES OF X
1130 C          DE,BHP,DA,DR = AIRCRAFT CONTROLS
1140 C          DETRM,BHPTRM,ETC. = TRIM SETTINGS FOR CONTROLS
1150 C          AKROOT,AKV,ETC. = AUTO PILOT CONTROL GAINS
1160 C          IX = VARIABLE OR CONTROL TO BE PLOTTED
1170 C          AUTO,VELC,PSIC = COMMANDS TO FLY (ALT,VEL,HEADING)
1180 C          TMAX = THE TIME LIMIT FOR THE INTEGRATION
1200 C          ALTSPEC(S) = SELECTION FOR LR (1), HP (2), BOTH (3)
1400 C          NSPP = NUMBER OF POINTS PLOTTED
1500 C          NPTS = CURRENT POINT NUMBER COUNTER
1600 C          NDIM = 12, THE DIMENSION OF X AND DX
1700 C          ICNT = CURRENT LOOP NUMBER COUNTER
1810 C          XP = ARRAY STORING THE DESIRED X POINTS
1900 C          TP = ARRAY STORING THE DESIRED T POINTS
2000 C *****
2100 C *****
2200 C          DIMENSION X(12),DX(12),ERR(12),XP(1,250),TP(1,250),ALTSPEC(5)
2300 C          CHARACTER*60 TITLE(4),XTITLE(4),LABEL(4),VLINE(4),LINE(4),TLINE(4)
2400 C          COMMON /BLK12/ DBN,ALON,CLON,AVEL,AC,LOTCODE,CMD,CMA,CMAO,CMD,
2500 C          1             CMCE,CYB,CYR,CYS,CYOR,CYB,CYR,CYOR,CYB,CYR,CYOR,CYB,
2600 C          2             CNR,CNR,CNR,CNR,CNR,CNR,CNR,CNR,CNR,CNR,CNR,CNR,
2700 C          3             CA,DE,DR,BHA
2800 C          DATA LABEL(4) / 'X', 'Y', 'Z', 'H' /
2900 C          DATA XTITLE(4) / 'TIME', 'X', 'Y', 'Z' /
3000 C          DATA TITLE(4) / 'STATE', 'E', 'V', 'A' /
3100 C *****
3200 C *****
3300 C          POINT IN THE DATA
3400 C *****
3500 C          READ(4) *
3600 C          READ(5) * DBN,ALON,CLON,AVEL,AC,LOTCODE,CMD,CMA,CMAO,CMD,
3700 C          1             CMCE,CYB,CYR,CYS,CYOR,CYB,CYR,CYOR,CYB,CYR,CYOR,CYB,
3800 C          2             CNR,CNR,CNR,CNR,CNR,CNR,CNR,CNR,CNR,CNR,CNR,CNR,
3900 C          3             CA,DE,DR,BHA
4000 C          READ(6) *
4100 C          READ(7) *
4200 C          READ(8) *
4300 C          READ(9) *
4400 C          READ(10) *
4500 C          READ(11) *
4600 C          READ(12) *
4700 C          READ(13) *
4800 C          READ(14) *
4900 C          READ(15) *
5000 C          READ(16) *
5100 C          READ(17) *
5200 C          READ(18) *
5300 C          READ(19) *
5400 C          READ(20) *
5500 C          READ(21) *
5600 C          READ(22) *
5700 C          READ(23) *
5800 C          READ(24) *
5900 C          READ(25) *
6000 C          READ(26) *
6100 C          READ(27) *
6200 C          READ(28) *
6300 C          READ(29) *
6400 C          READ(30) *
6500 C          READ(31) *
6600 C          READ(32) *
6700 C          READ(33) *
6800 C          READ(34) *
6900 C          READ(35) *
7000 C          READ(36) *
7100 C          READ(37) *
7200 C          READ(38) *
7300 C          READ(39) *
7400 C          READ(40) *
7500 C          READ(41) *
7600 C          READ(42) *
7700 C          READ(43) *
7800 C          READ(44) *
7900 C          READ(45) *
8000 C          READ(46) *
8100 C          READ(47) *
8200 C          READ(48) *
8300 C          READ(49) *
8400 C          READ(50) *
8500 C          READ(51) *
8600 C          READ(52) *
8700 C          READ(53) *
8800 C          READ(54) *
8900 C          READ(55) *
9000 C          READ(56) *
9100 C          READ(57) *
9200 C          READ(58) *
9300 C          READ(59) *
9400 C          READ(60) *
9500 C          READ(61) *
9600 C          READ(62) *
9700 C          READ(63) *
9800 C          READ(64) *
9900 C          READ(65) *

```

APPENDIX D- Simulation Program

This nonlinear simulation program was written in FORTRAN 77 for the Burroughs 6900 computer at the Air Force Academy by Cadet First Class Daniel A. Draeger. The program numerically integrates the six aircraft equations of motion for u , v , and w (velocity components in body axes) and for p , q , and r (rotational rates in body axes). Six kinematic equations are also integrated to get the Euler angles ϕ , θ , and ψ ; and displacements in the earth axes: altitude (h), north distance (N), and east distance (E). The results of simulation runs are delivered in graphical form using plotting routines not included in the listing. The aircraft data are read in from separate data files, a feature which allows the program to be used to simulate other aircraft. The twelve equations solved by the program are listed below in general form (Reference 1).

$m(\dot{u} - v r + w q) = \text{forces in x direction}$
 $m(\dot{v} + u r - w p) = \text{forces in y direction}$
 $m(\dot{w} - u q + v p) = \text{forces in z direction}$

$I_{xx}\dot{p} - I_{xz}\dot{r} - I_{xz}pq + (I_{zz} - I_{yy})rq = \text{moment about x axis}$

$I_{yy}\dot{q} + (I_{xx} - I_{zz})pr + I_{xz}(p^2 - r^2) = \text{moment about y axis}$

$I_{zz}\dot{r} - I_{xz}\dot{p} + (I_{yy} - I_{xx})pq + I_{xz}qr = \text{moment about z axis}$

$\phi = \phi_0 \sin \omega t + \phi_0 \cos \omega t$ sec
 $\theta = \theta_0 \cos \omega t + \theta_0 \sin \omega t$
 $\psi = \psi_0 \sin \omega t + \psi_0 \cos \omega t$

$h = h_0 \sin \omega t + h_0 \cos \omega t$
 $N = N_0 \sin \omega t + N_0 \cos \omega t$
 $E = E_0 \sin \omega t + E_0 \cos \omega t$

$$Y_B = \frac{\bar{q}_1 SC_{y_B}}{m} \text{ (ft sec}^{-2}\text{)}$$

$$Y_P = \frac{\bar{q}_1 SbC_{y_P}}{2mU_1} \text{ (ft sec}^{-1}\text{)}$$

$$Y_R = \frac{\bar{q}_1 SbC_{y_R}}{2mU_1} \text{ (ft sec}^{-1}\text{)}$$

$$Y_{\delta_a} = \frac{\bar{q}_1 SC_{y_{\delta_a}}}{m} \text{ (ft sec}^{-2}\text{deg}^{-1}\text{)}$$

$$Y_{\delta_r} = \frac{\bar{q}_1 SC_{y_{\delta_r}}}{m} \text{ (ft sec}^{-2}\text{deg}^{-1}\text{)}$$

$$L_B = \frac{\bar{q}_1 SbC_{L_B}}{I_{xx}} \text{ (sec}^{-2}\text{)}$$

$$L_P = \frac{\bar{q}_1 Sb^2 C_{L_P}}{2I_{xx}U_1} \text{ (sec}^{-1}\text{)}$$

$$L_R = \frac{\bar{q}_1 Sb^2 C_{L_R}}{2I_{xx}U_1} \text{ (sec}^{-1}\text{)}$$

$$L_{\delta_a} = \frac{\bar{q}_1 SbC_{L_{\delta_a}}}{I_{xx}} \text{ (sec}^{-2}\text{deg}^{-1}\text{)}$$

$$L_{\delta_r} = \frac{\bar{q}_1 SbC_{L_{\delta_r}}}{I_{xx}} \text{ (sec}^{-2}\text{deg}^{-1}\text{)}$$

$$N_B = \frac{\bar{q}_1 SbC_{n_B}}{I_{zz}} \text{ (sec}^{-2}\text{)}$$

$$N_{T_B} = \frac{\bar{q}_1 StC_{n_{T_B}}}{I_{zz}} \text{ (sec}^{-2}\text{)}$$

$$N_P = \frac{\bar{q}_1 Sb^2 C_{n_P}}{2I_{zz}U_1} \text{ (sec}^{-1}\text{)}$$

$$N_R = \frac{\bar{q}_1 Sb^2 C_{n_R}}{2I_{zz}U_1} \text{ (sec}^{-1}\text{)}$$

$$N_{\delta_a} = \frac{\bar{q}_1 SbC_{n_{\delta_a}}}{I_{zz}} \text{ (sec}^{-2}\text{deg}^{-1}\text{)}$$

$$N_{\delta_r} = \frac{\bar{q}_1 SbC_{n_{\delta_r}}}{I_{zz}} \text{ (sec}^{-2}\text{deg}^{-1}\text{)}$$

From Reference 1, the linearized lateral-directional equations of motion are (using the definitions from Table C-2):

$$U_1 \dot{\beta} + U_1 r = g \dot{\varphi} + Y_{\beta} \beta + Y_p p + Y_r r + Y_{\delta_a} \delta_a + Y_{\delta_r} \delta_r$$

$$\dot{p} - A_1 \dot{r} = L_{\beta} \beta + L_p p + L_r r + L_{\delta_a} \delta_a + L_{\delta_r} \delta_r$$

$$\dot{r} - B_1 \dot{p} = N_{\beta} \beta + N_T \beta + N_p p + N_r r + N_{\delta_a} \delta_a + N_{\delta_r} \delta_r$$

$$A_1 = \frac{I_{xz}}{I_{xx}}, \quad B_1 = \frac{I_{xz}}{I_{zz}}$$

In addition, the following approximations were added:

$$\begin{aligned} \dot{\varphi} &= p \\ \dot{\psi} &= r \end{aligned}$$

The values were substituted in and the equations were manipulated algebraically to obtain first order matrix form.

$$\begin{bmatrix} \dot{\beta} \\ \dot{p} \\ \dot{r} \\ \dot{\varphi} \\ \dot{\psi} \end{bmatrix} = \begin{bmatrix} -.5366 & -.000278 & -.9875 & .439 & 0 \\ -38.18 & -8.55 & 2.41 & 0 & 0 \\ 16.7 & .72 & -.448 & 0 & 0 \\ 0 & 1 & 0 & 0 & 0 \\ 0 & 0 & 1 & 0 & 0 \end{bmatrix} \begin{bmatrix} \beta \\ p \\ r \\ \varphi \\ \psi \end{bmatrix} + \begin{bmatrix} 0 & .00274 \\ 10.14 & .48 \\ -1.17 & -.157 \\ 0 & 0 \end{bmatrix} \begin{bmatrix} \delta_a \\ \delta_r \end{bmatrix}$$

Table C-1

$$x_u = \frac{-\bar{q}_1 S (C_{D_u} + 2C_{D_1})}{m U_1} (\text{sec}^{-1})$$

$$x_{T_u} = \frac{\bar{q}_1 S (C_{T_{x_u}} + 2C_{T_{x_1}})}{m U_1} (\text{sec}^{-1})$$

$$x_\alpha = \frac{-\bar{q}_1 S (C_{D_\alpha} - C_{L_1})}{m} (\text{ft sec}^{-2})$$

$$x_{\delta_e} = \frac{-\bar{q}_1 S C_{D_{\delta_e}}}{m} (\text{ft sec}^{-2} \text{deg}^{-1})$$

$$z_u = - \frac{\bar{q}_1 S (C_{L_u} + 2C_{L_1})}{m U_1} (\text{sec}^{-1})$$

$$z_\alpha = - \frac{\bar{q}_1 S (C_{L_\alpha} + C_{D_1})}{m} (\text{ft sec}^{-2})$$

$$z_{\dot{\alpha}} = - \frac{\bar{q}_1 S C_{L_{\dot{\alpha}}} \bar{c}}{2m U_1} (\text{ft sec}^{-1})$$

$$z_q = - \frac{\bar{q}_1 S C_{L_q} \bar{c}}{2m U_1} (\text{ft sec}^{-1})$$

$$z_{\delta_e} = - \frac{\bar{q}_1 S C_{L_{\delta_e}}}{m} (\text{ft sec}^{-2} \text{deg}^{-1})$$

$$M_u = \frac{\bar{q}_1 S \bar{c} (C_{m_u} + 2C_{m_1})}{I_{yy} U_1} (\text{ft}^{-1} \text{sec}^{-1})$$

$$M_{T_u} = \frac{\bar{q}_1 S \bar{c} (C_{m_{T_u}} + 2C_{m_{T_1}})}{I_{yy} I_1} (\text{ft}^{-1} \text{sec}^{-1})$$

$$M_\alpha = \frac{\bar{q}_1 S \bar{c} C_{m_\alpha}}{I_{yy}} (\text{sec}^{-2})$$

$$M_{T_\alpha} = \frac{\bar{q}_1 S \bar{c} C_{m_{T_\alpha}}}{I_{yy}} (\text{sec}^{-2})$$

$$\dot{M}_\alpha = \frac{\bar{q}_1 S \bar{c}^2 C_{m_\alpha}}{2I_{yy} U_1} (\text{sec}^{-1})$$

$$M_q = \frac{\bar{q}_1 S \bar{c}^2 C_{m_q}}{2I_{yy} U_1} (\text{sec}^{-1})$$

$$M_{\delta_e} = \frac{\bar{q}_1 S \bar{c} C_{m_{\delta_e}}}{I_{yy}} (\text{sec}^{-2} \text{deg}^{-1})$$

$$x_{T_{\delta_T}} = \frac{\bar{q}_1 S C_{T_{x_{\delta_T}}}}{m} (\text{ft sec}^{-2} \text{BHP}^{-1})$$

The remaining necessary coefficients and derivatives, listed below, were obtained by linearizing the drag polar around the steady-state condition and by assuming that the propeller thrust acts through the aircraft center of gravity.

$$\begin{aligned} C_{D_1} &= .073 & C_{m_1} &= 0 & C_{T_{x_1}} &= .073 \\ C_{D_\alpha} &= .259/\text{rad} & C_{m_{T_1}} &= 0 \\ C_{L_1} &= .376 & C_{m_{T_\alpha}} &= 0 \end{aligned}$$

From Reference 1, the linearized longitudinal equations of motion are (using the definitions from Table C-1):

$$\dot{U} = -g\theta + X_U U + X_{T_U} U + X_\alpha \alpha + X_{\delta_e} \delta_e + X_{T_{\delta_T}} \delta_T$$

$$U_1 \dot{\alpha} - U_1 q = Z_U U + Z_\alpha \alpha + Z_{\dot{\alpha}} \dot{\alpha} + Z_q q + Z_{\delta_e} \delta_e$$

$$\dot{q} = M_U U + M_{T_U} U + M_\alpha \alpha + M_{T_\alpha} \alpha + M_{\dot{\alpha}} \dot{\alpha} + M_q q + M_{\delta_e} \delta_e$$

In addition, the following approximations were added:

$$\dot{\theta} = q$$

$$\dot{h} = U_1 \theta - U_1 \alpha$$

The values were substituted in and the equations were manipulated algebraically to obtain first order matrix form.

$$\begin{bmatrix} \dot{q} \\ \dot{\theta} \\ \dot{U} \\ \dot{\alpha} \\ \dot{h} \end{bmatrix} = \begin{bmatrix} -3.733 & 0 & .01189 & -1.341 & 0 \\ 1 & 0 & 0 & 0 & 0 \\ 0 & -32.2 & -.2566 & 10.01 & 0 \\ .9193 & 0 & -.01169 & -4.642 & 0 \\ 0 & 73.33 & 0 & -73.33 & 0 \end{bmatrix} \begin{bmatrix} q \\ \theta \\ U \\ \alpha \\ h \end{bmatrix} + \begin{bmatrix} -.2033 & 0 \\ 0 & 0 \\ -.0257 & 5.63 \\ -.0057 & 0 \\ 0 & 0 \end{bmatrix} \begin{bmatrix} \delta_e \\ \delta_T \end{bmatrix}$$

3. Estimated Aerodynamic Data (Reference 1 and 5):

$$C_{m_u} = C_{L_u} = C_{D_u} = C_{m_{T_u}} = C_{m_{T_\alpha}} = 0$$

$$C_{m_{\dot{\alpha}}} = -4.0$$

$$C_{n_{T_\beta}} = 0$$

$$C_{m_q} = -11.0$$

$$C_{n_r} = -.046$$

$$C_{L_{\dot{\alpha}}} = 1.66$$

$$C_{n_p} = -.03$$

$$C_{L_q} = 4.16$$

$$C_{\ell_\beta} = -.078/\text{rad}^*$$

$$C_{T_{x_u}} = -.22$$

$$C_{\ell_p} = -.36$$

$$C_{y_p} = -.004$$

$$C_{\ell_r} = .096$$

$$C_{y_r} = .18$$

$$C_{T_{x_{\delta_T}}} = .066/\text{BHP}$$

*wind tunnel data not used because model had no wing dihedral

4. Mass Data (Reference 4):

$$\text{rolling moment of inertia } (I_{xx}) = 1.7 \text{ slg-ft}^2$$

$$\text{pitching moment of inertia } (I_{yy}) = 6.8 \text{ slg-ft}^2$$

$$\text{yawing moment of inertia } (I_{zz}) = 9.3 \text{ slg-ft}^2$$

$$\text{product of inertia } (I_{xz}) = 0$$

note: these inertia terms are relative to body axes

APPENDIX C- Aircraft Linearized Equations of Motion

The methods of Reference 1 were used to linearize the aircraft equations of motion about a steady-state condition of coordinated, straight and level flight at 7500 feet and 73.33 ft/s (50 mph). The angle of attack required for this condition was 7.2 degrees relative to body axes. Since the linearized model uses stability axes (longitudinal axis parallel to the steady-state relative wind), the inertia terms I_{xx} , I_{zz} , and I_{xz} , of Appendix B had to be transformed from body axes to stability axes.

-1.128241961 J 0
 -.915390605 J -.551649739
 -.915390605 J .551649739
 -1.91013555 J 0
 -5.24272001 J 0

KHD = -.2 DEG / FT/SEC
 KH = .2 FT/SEC / FT
 KV = .1 BHP / FT/SEC
 1 S**5 + 9.11187873 S**4 + 25.3997775 S**3 + 29.6077331 S**2 + 15.5221765 S + 1.95593185

POLES ARE:

-2.00669996 J 0
 -5.23439389 J 0
 -.846614841 J -.57618756
 -.846614841 J .57618756
 -.177555202 J 0

KHD = -.2 DEG / FT/SEC
 KH = .25 FT/SEC / FT
 KV = .1 BHP / FT/SEC
 1 S**5 + 9.11187873 S**4 + 25.3955989 S**3 + 29.6009527 S**2 + 16.2064611 S + 2.44491481

POLES ARE:

-2.08932918 J 0
 -5.22595506 J 0
 -.783362962 J -.00383671
 -.783362962 J .00383671
 -.229868565 J 0

KHD = -.2 DEG / FT/SEC
 KH = .3 FT/SEC / FT
 KV = .1 BHP / FT/SEC
 1 S**5 + 9.11187873 S**4 + 25.3914204 S**3 + 29.5941724 S**2 + 16.8907457 S + 2.93389777

POLES ARE:

-2.16250743 J 0
 -5.21739973 J 0
 -.724015404 J -.625789061
 -.724015404 J .625789061
 -.280940771 J 0

KHD = -.2 DEG / FT/SEC
 KH = .2 FT/SEC / FT
 KV = .04 BHP / FT/SEC
 1 S**5 + 8.77316074 S**4 + 22.5915516 S**3 + 23.3513994 S**2 + 10.872586 S + 1.02599105

POLES ARE:

-1.123213703 1 0
-1.720633944 1 -1.535506228
-1.720633944 1 .535506228
-1.97301432 1 0
-5.23566482 1 0

KHD = -.2 DEG / FT/SEC

KH = .2 FT/SEC / FT

KV = .06 BHP / FT/SEC

1 S**5 + 8.88606673 S**4 + 23.5276269 S**3 + 25.436844 S**2 + 12.4255646 S + 1.33596465

POLES ARE:

-1.145187511 1 0
-1.761329061 1 -1.553845598
-1.761329061 1 .553845598
-1.98295914 1 0
-5.23526197 1 0

KHD = -.2 DEG / FT/SEC

KH = .2 FT/SEC / FT

KV = .06 BHP / FT/SEC

1 S**5 + 8.99897273 S**4 + 24.4637022 S**3 + 27.5222885 S**2 + 13.9738705 S + 1.64594825

POLES ARE:

-1.9941163 1 0
-5.23483885 1 0
-1.803528034 1 -1.56736352
-1.803528034 1 .56736352
-1.162961521 1 0

KHD = -.2 DEG / FT/SEC

KH = .2 FT/SEC / FT

KV = .1 BHP / FT/SEC

1 S**5 + 9.11187677 S**4 + 25.3597775 S**3 + 29.6077331 S**2 + 15.5221765 S + 1.95593185

POLES ARE:

-2.00664997 1 0
-5.103429263 1 0
-1.846614619 1 -1.576187561
-1.846614619 1 .576187561
-1.177505202 1 0

KHD = -.2 DEG / FT/SEC

KH = .2 FT/SEC / FT

KV = .12 BHP / FT/SEC

1 S**5 + 9.01418473 S**4 + 26.7258527 S**3 + 31.5931176 S**2 + 14.0704824 S + 2.26591545

FOLES ARE:

-5.8008353 J -580455601
-5.89083331 J -580455601
-5.23392534 J 0
-2.12007073 J 0
-1.18704689 J 0

KH = 1.2 DEG / FT/SEC

KH = 1.2 FT/SEC / FT

KV = 1.14 BHP / FT/SEC

1.5**5 + 9.33769073 S**4 + 27.271928 S**3 + 33.7786222 S**2 + 16.6187683 S + 2.57589904

FOLES ARE:

-5.93352349 J -580293241
-5.93352349 J -580293241
-5.2334311 J 0
-2.33714597 J 0
-1.144966766 J 0

KH = 1.2 DEG / FT/SEC

KH = 1.2 FT/SEC / FT

KV = 1.15 BHP / FT/SEC

1.5**5 + 9.45059674 S**4 + 26.2080033 S**3 + 35.8640668 S**2 + 20.1670943 S + 2.68588265

FOLES ARE:

-5.23290956 J 0
-5.976525123 J -575809024
-5.976525123 J -575809024
-2.05591145 J 0
-1.20872506 J 0

Lateral-directional Poles

KNY = 0 DEG/s
KR = 0 DEG/RAD/S
KPSI = 0 RAD/S/RAD
KYD = 0 DEG/RAD/S
1 S**5 + 9.5346 S**4 + 23.4041628 S**3 + 131.745946 S**2 + -10.159496 S + 0

POLES ARE:

.0760546455 j 0
-1.500580503 j -3.90704845
-1.500580503 j 3.90704845
-8.60949365 j 0
0 j 0

KNY = 0 DEG/s
KR = 1 DEG/RAD/S
KPSI = .1 RAD/S/RAD
KYD = -20 DEG/RAD/S
1 S**5 + 11.5046 S**4 + 40.6514048 S**3 + 134.318141 S**2 + 26.6701227 S + 5.47289886

POLES ARE:

-8.54374773 j 0
-1.38137235 j -3.58688741
-1.38137235 j 3.58688741
-0.990537396 j -1.183157467
-0.990537396 j 1.183157467

KNY = 1 DEG/s
KR = 1 DEG/RAD/S
KPSI = .1 RAD/S/RAD
KYD = 1 DEG/RAD/S
1 S**5 + 11.627947 S**4 + 44.659137 S**3 + 150.239301 S**2 + 30.1706699 S + 8.06247998

POLES ARE:

-0.990537396 j 0
-0.990537396 j -1.183157467
-0.990537396 j 1.183157467
-0.990537396 j -1.183157467
-0.990537396 j 1.183157467

KNY = 2 DEG/s

KR = 1 DEG/RAD/S

KPSI = .1 RAD/S/RAD

KYD = 1 DEG/RAD/S

1 S**5 + 12.1375451 S**4 + 47.2770816 S**3 + 168.404667 S**2 + 34.1706547 S + 8.71616742

POLES ARE:

-8.64578947 j 0
-1.64450809 j -3.95216212
-1.64450809 j 3.95216212
-.101569701 j -.179452201
-.101569701 j .179452201

KNY = 30 DEG/s

KR = 1 DEG/RAD/S

KPSI = .1 RAD/S /RAD

KYD = 20 DEG/RAD/S

1 S**5 + 11.5075614 S**4 + 54.4966084 S**3 + 189.418558 S**2 + 38.7851716 S + 7.51334065

POLES ARE:

-8.21027749 j 0
-1.80600033 j -4.14745607
-1.80600033 j 4.14745607
-.10266164 j -.177803379
-.10266164 j .177803379

KNY = 40 DEG/s

KR = 1 DEG/RAD/S

KPSI = .1 RAD/S /RAD

KYD = 20 DEG/RAD/S

1 S**5 + 11.9610645 S**4 + 60.8427901 S**3 + 213.897442 S**2 + 44.1676258 S + 8.41982831

POLES ARE:

-8.06719367 j 0
-1.49717102 j 4.15186056
-1.49717102 j 4.15186056
-.10166163 j -.176871479
-.10166163 j .176871479

KNY = 50 DEG/s

KR = 1 DEG/RAD/S

KPSI = .1 RAD/S /RAD

KYD = 20 DEG/RAD/S

1 S**5 + 13.5188797 S**4 + 67.9042413 S**3 + 242.818953 S**2 + 50.5271121 S + 9.49083428

POLES ARE:

-8.68081769 j 0
-2.11444504 j 4.50544296
-2.11444504 j 4.50544296
-.104781131 j -.174847122
-.104781131 j .174847122

KNY = 60 DEG/s

KR = 1 DEG/RAD/S

KPI = 1.1 RAD S RAD
 KPI = 1.1 RAD S RAD S
 1.5**5 + 14.1515127 S**4 + 76.5145123 S**3 + 277.513.18 S**2 + 58.156.149 S + 10.775616

POLLS ARE:
 -8.9915778 j 0
 -2.4712136y j -4.76718744
 -3.47226309 j 4.76718744
 -1.05429185 j -1.173509154
 -1.05429185 j 1.173509154

KPI = 1.0 DEB RAD S
 KPI = 1.1 RAD S RAD
 KPI = 1.1 DEB RAD S
 1.5**5 + 11.9955614 S**4 + 55.9236229 S**3 + 190.287321 S**2 + 8.89488741 S + 4.50600439

POLLS ARE:
 -1.44121 j 0
 -1.95144 j 4.11124402
 -1.95144 j 4.11124402
 -1.919951268 j -1.153661036
 -1.919951268 j 1.153661036

KPI = 1.0 DEB
 KPI = 1.0 DEB RAD S
 KPI = 1.1 RAD S RAD
 KPI = 1.0 DEB RAD S
 1.5**5 + 12.7515614 S**4 + 55.0102156 S**3 + 189.85297 S**2 + 23.7950296 S + 6.01067252

POLLS ARE:
 -3.92673673 j 0
 -1.89720673 j -4.17997346
 -1.89720673 j 4.17997346
 -1.09255227 j -1.170952076
 -1.09255227 j 1.170952076

KPI = 1.0 DEB
 KPI = 1.0 DEB RAD S
 KPI = 1.1 RAD S RAD
 KPI = 1.0 DEB RAD S
 1.5**5 + 11.17794 S**4 + 4.43564 S**3 + 15.416156 S**2 + 16.157718 S + 1.5131465

POLLS ARE:
 -1.171274 j 0
 -1.171274 j 1.171274
 -1.171274 j 1.171274
 -1.171274 j 1.171274

[illegible]

1. 10. 1950	1. 10. 1950
2. 10. 1950	2. 10. 1950
3. 10. 1950	3. 10. 1950
4. 10. 1950	4. 10. 1950
5. 10. 1950	5. 10. 1950
6. 10. 1950	6. 10. 1950
7. 10. 1950	7. 10. 1950
8. 10. 1950	8. 10. 1950
9. 10. 1950	9. 10. 1950
10. 10. 1950	10. 10. 1950
11. 10. 1950	11. 10. 1950
12. 10. 1950	12. 10. 1950
13. 10. 1950	13. 10. 1950
14. 10. 1950	14. 10. 1950
15. 10. 1950	15. 10. 1950
16. 10. 1950	16. 10. 1950
17. 10. 1950	17. 10. 1950
18. 10. 1950	18. 10. 1950
19. 10. 1950	19. 10. 1950
20. 10. 1950	20. 10. 1950
21. 10. 1950	21. 10. 1950
22. 10. 1950	22. 10. 1950
23. 10. 1950	23. 10. 1950
24. 10. 1950	24. 10. 1950
25. 10. 1950	25. 10. 1950
26. 10. 1950	26. 10. 1950
27. 10. 1950	27. 10. 1950
28. 10. 1950	28. 10. 1950
29. 10. 1950	29. 10. 1950
30. 10. 1950	30. 10. 1950
31. 10. 1950	31. 10. 1950
1. 11. 1950	1. 11. 1950
2. 11. 1950	2. 11. 1950
3. 11. 1950	3. 11. 1950
4. 11. 1950	4. 11. 1950
5. 11. 1950	5. 11. 1950
6. 11. 1950	6. 11. 1950
7. 11. 1950	7. 11. 1950
8. 11. 1950	8. 11. 1950
9. 11. 1950	9. 11. 1950
10. 11. 1950	10. 11. 1950
11. 11. 1950	11. 11. 1950
12. 11. 1950	12. 11. 1950
13. 11. 1950	13. 11. 1950
14. 11. 1950	14. 11. 1950
15. 11. 1950	15. 11. 1950
16. 11. 1950	16. 11. 1950
17. 11. 1950	17. 11. 1950
18. 11. 1950	18. 11. 1950
19. 11. 1950	19. 11. 1950
20. 11. 1950	20. 11. 1950
21. 11. 1950	21. 11. 1950
22. 11. 1950	22. 11. 1950
23. 11. 1950	23. 11. 1950
24. 11. 1950	24. 11. 1950
25. 11. 1950	25. 11. 1950
26. 11. 1950	26. 11. 1950
27. 11. 1950	27. 11. 1950
28. 11. 1950	28. 11. 1950
29. 11. 1950	29. 11. 1950
30. 11. 1950	30. 11. 1950
31. 11. 1950	31. 11. 1950
1. 12. 1950	1. 12. 1950
2. 12. 1950	2. 12. 1950
3. 12. 1950	3. 12. 1950
4. 12. 1950	4. 12. 1950
5. 12. 1950	5. 12. 1950
6. 12. 1950	6. 12. 1950
7. 12. 1950	7. 12. 1950
8. 12. 1950	8. 12. 1950
9. 12. 1950	9. 12. 1950
10. 12. 1950	10. 12. 1950
11. 12. 1950	11. 12. 1950
12. 12. 1950	12. 12. 1950
13. 12. 1950	13. 12. 1950
14. 12. 1950	14. 12. 1950
15. 12. 1950	15. 12. 1950
16. 12. 1950	16. 12. 1950
17. 12. 1950	17. 12. 1950
18. 12. 1950	18. 12. 1950
19. 12. 1950	19. 12. 1950
20. 12. 1950	20. 12. 1950
21. 12. 1950	21. 12. 1950
22. 12. 1950	22. 12. 1950
23. 12. 1950	23. 12. 1950
24. 12. 1950	24. 12. 1950
25. 12. 1950	25. 12. 1950
26. 12. 1950	26. 12. 1950
27. 12. 1950	27. 12. 1950
28. 12. 1950	28. 12. 1950
29. 12. 1950	29. 12. 1950
30. 12. 1950	30. 12. 1950
31. 12. 1950	31. 12. 1950

$$-0.7968 \times 10^{-1} + 51.422664 \text{ G**}^3 + 169.349537 \text{ G**}^2 + 78.748536 \text{ S} + 9.01870876$$
[illegible][illegible]

1. The first part of the document is a list of the names of the persons who were present at the meeting. The names are listed in alphabetical order.

2. The second part of the document is a list of the names of the persons who were present at the meeting. The names are listed in alphabetical order.

3. The third part of the document is a list of the names of the persons who were present at the meeting. The names are listed in alphabetical order.

4. The fourth part of the document is a list of the names of the persons who were present at the meeting. The names are listed in alphabetical order.

5. The fifth part of the document is a list of the names of the persons who were present at the meeting. The names are listed in alphabetical order.

6. The sixth part of the document is a list of the names of the persons who were present at the meeting. The names are listed in alphabetical order.

7. The seventh part of the document is a list of the names of the persons who were present at the meeting. The names are listed in alphabetical order.

8. The eighth part of the document is a list of the names of the persons who were present at the meeting. The names are listed in alphabetical order.

76

77

78

79

80

END

FILMED

7-35

DTIC